

Recent Developments on the CKM Matrix

Wei Wang

*INPAC, Department of Physics and Astronomy, Shanghai Jiao Tong University, Shanghai,
 200240, P. R. China*

and

*Helmholtz-Institut für Strahlen- und Kernphysik, Universität Bonn, Bonn 53115, Germany
 weiwang@hiskp.uni-bonn.de*

Received xxx

Accepted xxx

Published xxx

.pdf

In Standard Model, CP violation arises from an irreducible complex phase in the quark mixing matrix, now under the name Cabibbo-Kobayashi-Maskawa matrix. This description has shown remarkably overall agreement with various experimental measurements. In this review, we discuss recent experimental data and theoretical developments on three quantities of CKM matrix that are most uncertain: the V_{ub} , including its magnitude and the phase γ in standard parametrization, and the $B_s - \bar{B}_s$ mixing phase β_s .

Keywords: CKM matrix; B-meson decays; QCD

PACS numbers: 12.15.Hh, 13.20.He, 13.25.Hw

Contents

1. Introduction	2
2. $ V_{ub} $	4
2.1. Inclusive decays	6
2.2. Exclusive decays $B \rightarrow \pi \ell \bar{\nu}$	7
2.3. Other Semi-Leptonic B decay modes	8
2.4. Purely leptonic decays	9
2.5. Theoretical developments on multi-body semileptonic B decays	11
3. γ	16
3.1. CP violation effects and errors in $B \rightarrow DK$	17
3.2. Experimental results	19
3.3. B decays into a scalar/tesnor state	19
3.4. Three-body B decays	21
4. β_s	21
5. Summary and Outlook	24

1. Introduction

In the Standard Model (SM) of particle physics the three observed generations of quarks show a remarkable feature that their weakly interacting eigenstates do not coincide with their mass eigenstates. This “misalignment” gives rise to flavor changing transitions that can be represented by a 3×3 mixing matrix. The mixing scheme was formulated first by Cabibbo¹ for two generations, and extended later to three generations by Kobayashi and Maskawa,² now referred to as the Cabibbo-Kobayashi-Maskawa (CKM) matrix. In this unitary 3×3 matrix, there is an irreducible complex phase, which can give rise to a difference in the decays of a particle and its antiparticle, namely CP violation.

In the SM, all flavour-changing interactions of quarks, from the lowest energies (such as nuclear transitions and pion decays) to the highest energies that can be reached at high energy accelerators for instance the Large Hadron Collider (LHC), are described by four parameters of the CKM matrix, which makes it a remarkably predictive paradigm. However new physics (NP) degrees of freedom are generally believed to exist at the TeV scale or not too much higher, and may show patterns deviating from the CKM mechanism. Thus a precise determination of CKM parameters is not only useful for the test of SM but can also serve as an indirect probes for the NP.

The CKM matrix^{1,2} describes the mixing between the three families of quarks. Thereby it is a 3×3 unitary matrix, and can be parametrized in terms of four real parameters. For example, in Wolfenstein parametrisation³ it can be expressed as

$$\begin{aligned} V_{\text{CKM}} &= \begin{pmatrix} V_{ud} & V_{us} & V_{ub} \\ V_{cd} & V_{cs} & V_{cb} \\ V_{td} & V_{ts} & V_{tb} \end{pmatrix} \\ &= \begin{pmatrix} 1 - \frac{\lambda^2}{2} & \lambda & A\lambda^3(\rho - i\eta) \\ -\lambda & 1 - \frac{\lambda^2}{2} & A\lambda^2 \\ A\lambda^3(1 - \rho - i\eta) & -A\lambda^2 & 1 \end{pmatrix} + \mathcal{O}(\lambda^4), \end{aligned} \quad (1)$$

where the expansion parameter λ is the sine of the Cabibbo angle. The diagonal elements are of unity, but an empirical relation exists for the off-diagonal elements^a:

$$|V_{ij}| \sim \lambda^{\max(i,j)+|i-j|-2}, \quad (2)$$

where i, j is the family index. With four independent parameters, a 3×3 unitary matrix cannot be forced to be real-valued, and hence CP violation arises as a consequence of the fact that the couplings for quarks and antiquarks have different phases, *i.e.* $V_{\text{CKM}} \neq V_{\text{CKM}}^*$. In the SM, all CP violation in the quark sector indeed arises from this fact, which is encoded in the Wolfenstein parameter η .

In this review, we will concentrate on three quantities in the CKM matrix: the $|V_{ub}|$, the phase γ , and β_s , whose determinations are most uncertain nowadays

^aDue to the smallness of $|V_{ub}|$, it has been proposed for instance in Ref.⁴ that the $V_{ub} \sim \lambda^4$. I thank Prof. Zhi-Zhong Xing for an interesting discussion on this relation.

but have been greatly improved in the past a few years. Most precise results on the $|V_{ub}|$ arise from exclusive and inclusive semi-leptonic $b \rightarrow u$ decays, and see for instance Ref. ⁵⁻⁹ for recent reviews. These determinations rely on different theoretical calculations and on different experimental measurements which very likely have uncorrelated statistical and systematic uncertainties. The independence in these determinations from inclusive and exclusive decays makes the comparison of $|V_{ub}|$ a powerful test of the CKM mechanism.

The unitarity constraints on the CKM matrix can be represented as triangles in the complex plane: the lengths of whose sides are the moduli of CKM matrix element products, while the angles are constructed from the relative phases. For instance the orthogonality

$$V_{ud}V_{ub}^* + V_{cd}V_{cb}^* + V_{td}V_{tb}^* = 0, \quad (3)$$

form the commonly-studied (bd) unitarity triangle as shown in Fig. 1. The current global fitting results on this triangle by the CKMfitter,¹⁰ and UTfit Group,¹¹ and in the scan method¹² can be summarised in Fig. 2.

The three angles (α, β, γ) as shown in Fig. 1 satisfy the constraint, $\alpha + \beta + \gamma = 180^\circ$, that can be tested via experimental measurements. The world averages from Particle Data Group (PDG) in 2012 are given as⁹

$$\alpha = (89.0_{-4.2}^{+4.4})^\circ, \quad \text{PDG2012} \quad (4)$$

$$\gamma = (68_{-11}^{+10})^\circ, \quad \text{PDG2012} \quad (5)$$

while the result

$$\sin(2\beta) = (0.679 \pm 0.020) \quad \text{PDG2012} \quad (6)$$

has a four-fold ambiguity for the β angle. The error in γ is about 10° .⁹⁻¹³ Though it is one of the main sources of current uncertainties on the apex of the unitary triangle, recent measurements and theoretical investigations are progressing very fast and will be covered later in this review. With a large amount of data accumulated in the future, the LHCb would be able to diminish the errors in γ to about 4° from the $B \rightarrow DK$ until 2018, and to 1° after the upgrade.¹⁴ On the SuperB factories the error can be reduced to 2° .^{15,16}

In contrast with the (bd) triangle, the (bs) triangle, $V_{tb}V_{ts}^* + V_{cb}V_{cs}^* + V_{ub}V_{us}^* = 0$, has a much smaller complex phase:

$$\phi_s = (-0.036 \pm 0.002) \quad \text{rad}, \quad (7)$$

with $\phi_s = -2\beta_s = -2\arg[-V_{ts}V_{tb}^*/(V_{cs}V_{cb}^*)]$.¹⁷ The smallness of the β_s can provide a null test of the SM, and the observation of a large non-zero value would probably indicate a signal for NP beyond the SM. Previous data obtained by the CDF¹⁸ and D0¹⁹ collaborations, based on the angular analysis of $B_s \rightarrow J/\psi\phi$, indicate much larger values with sizeable uncertainties. This deviation from the SM value has been treated as signals of NP but is softened by new measurements in the physics programs at the LHC.

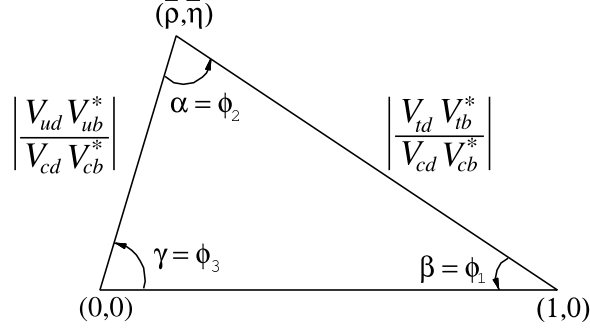


Fig. 1. A sketch of the bd unitary triangle formed by $V_{ud}V_{ub}^* + V_{cd}V_{cb}^* + V_{td}V_{tb}^* = 0$.

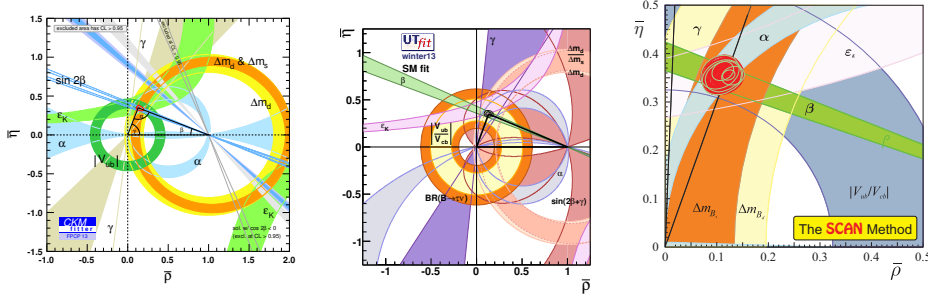


Fig. 2. Global fitting constraints on the (bd) unitary triangle from the CKMfitter Group,¹⁰ UTfit Group,¹¹ and the scan method.¹²

The rest of this review is organised as follows. Sec. 2 will discuss the extraction of the $|V_{ub}|$ from semi-leptonic and leptonic B decays. In this section, we will summarise the latest results from the experimental data on various channels, and give a look at the future prospect. At the same time, considerable focus will be spent on the recent developments of theoretical techniques that can be applied to multi-body semileptonic B decays like the $B \rightarrow \pi\pi\ell\bar{\nu}_\ell$. In Sec. 3, we will review the status on the angle γ , including the newly released experimental data and new theoretical insights. In Sec. 4, we will discuss the recent progress in the extraction of β_s through the $B_s \rightarrow J/\psi\phi$ and $B_s \rightarrow J/\psi f_0(980)$. We conclude in Sec. 5.

2. $|V_{ub}|$

As one can see from Fig. 1, the length of the side opposite the β angle is proportional to the $|V_{ub}|$ and thus its determination is of great importance. However since the $|V_{ub}|$ is the smallest matrix element, its determination has a limited precision:⁹

$$|V_{ub}| = \begin{cases} (4.41 \pm 0.15^{+0.15}_{-0.17}) \times 10^{-3} & \text{inclusive} \\ (3.23 \pm 0.31) \times 10^{-3} & \text{exclusive} \end{cases} \quad \text{PDG2012,} \quad (8)$$

where the errors are about 10%.

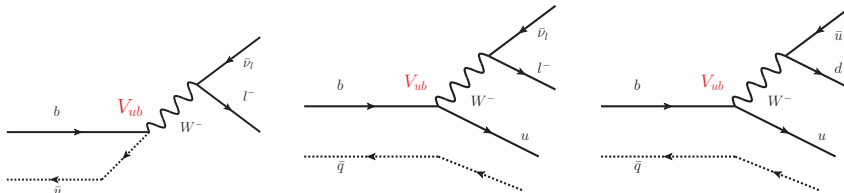


Fig. 3. Decay modes that can be used to extract the $|V_{ub}|$: purely leptonic (first panel), semi-leptonic (second panel) and non-leptonic B decays (last panel).

The magnitude $|V_{ub}|$ can be determined from a multitude of weak B -decays governed by the $b \rightarrow u$ transition which involve either inclusive or exclusive final states, whose Feynman diagrams are sketched in Fig. 3. These processes exhibit different experimental and theoretical challenges. Compared to leptonic and semi-leptonic decay modes, non-leptonic processes receive additional complexity due to the entanglement with the emitted hadron in final state, and thus its constraint on the $|V_{ub}|$ is quite uncertain (see Ref.²⁰ for a recent discussion).

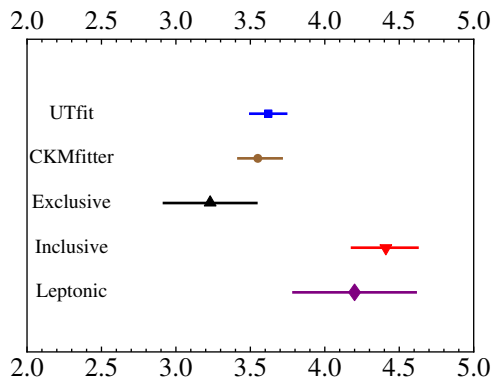


Fig. 4. $|V_{ub}|$ (in units of 10^{-3}) obtained from experimental data and the global fitting approach.

At the current stage, the increased precision has made manifest a tension between the values of $|V_{ub}|$ extracted from exclusive and inclusive semileptonic decays. As shown in Eq. (8), the inclusive determinations mostly yield a central value larger than 4×10^{-3} , while exclusive analyses produce central values below this. In Fig. 4, we have collected the results from exclusive and inclusive processes as shown in Eq. (8) together with the indirect fits^{10,11}

$$|V_{ub}| = (3.65 \pm 0.13) \times 10^{-3}, \quad \text{UTfit}, \quad (9)$$

$$|V_{ub}| = (3.49^{+0.21}_{-0.10}) \times 10^{-3}, \quad \text{CKMfitter}, \quad (10)$$

and the value from leptonic process later shown in Eq. (21). The global fit approaches prefer to a lower $|V_{ub}|$ that is closer to the exclusive determination, while the leptonic result is more consistent with the inclusive determination. Although the tension in $|V_{ub}|$ is only approximately 3σ , it has already created a significant amount of speculations about possible NP effects. See Ref.²¹ for a recent discussion.

2.1. Inclusive decays

By integrating the off-shell W boson out, one can obtain the effective Hamiltonian for the $b \rightarrow u\ell^-\bar{\nu}_\ell$ transition

$$\mathcal{H}_{\text{eff}} = \frac{G_F}{\sqrt{2}} V_{ub} \bar{u} \gamma_\mu (1 - \gamma_5) b \bar{\ell} \gamma^\mu (1 - \gamma_5) \nu_\ell + h.c., \quad (11)$$

with the Fermi constant G_F .

In inclusive decays $B \rightarrow X_u \ell \bar{\nu}_\ell$, X_u refers to the sum of all possible final states. The theoretical description of $B \rightarrow X_u \ell \bar{\nu}_\ell$ decays is based on heavy quark expansion, which has been validated in various studies. Two-loop $\mathcal{O}(\alpha_s^2)$ corrections have also been recently calculated, for instance, in Ref.²² Unfortunately, the total decay rate is very difficult to measure due to the large background from the $B \rightarrow X_c \ell \bar{\nu}_\ell$.

Theoretical calculation of the partial decay rate in the region where the $B \rightarrow X_c \ell \bar{\nu}_\ell$ is suppressed requests the knowledge of an unknown non-perturbative distribution function. The explicit realisations differ significantly in the treatment of perturbative corrections and the parameterization of non-perturbative effects.

The shape function approach^{23–25} is based on the introduction of shape function that at leading order is universal, and can be constrained from the $B \rightarrow X_s \gamma$. The shape function takes care of singular terms in the theoretical spectrum; it has the role of a momentum distribution function of the b -quark in the B meson. However, no prediction is available for the shape function and an ansatz is needed for its functional form. The subleading shape functions are not process independent and thus are difficult to constrain.

Predictions based on resummed perturbative QCD use resummed perturbation theory to provide a perturbative calculation of the on-shell decay spectrum in the entire phase space. It can extend the standard Sudakov resummation framework by adding non-perturbative corrections, whose structure is determined by renormalon resummung²⁶ or by an effective QCD coupling.^{27–29}

On the experimental side, efforts have been made to enlarge the experimental range, so as to reduce the weight of the endpoint region. Latest results by Belle³⁰ can access $\sim 90\%$ of the $\bar{B} \rightarrow X_u \ell \bar{\nu}_\ell$ phase space, claiming an overall uncertainty of 7% on $|V_{ub}|$. A similar portion of the phase space is also covered in recent BaBar analysis.³¹

Though conceptually different, all the above approaches can lead to consistent results when the same inputs are used, and this situation has been reviewed in Ref.^{5,6} The averaged values have been given in Eq. (8).

2.2. Exclusive decays $B \rightarrow \pi \ell \bar{\nu}$

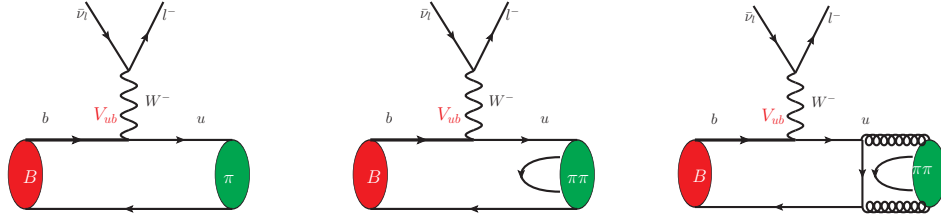


Fig. 5. Feynman diagrams for the $B \rightarrow \pi \ell \bar{\nu}$ (left panel) and $B \rightarrow \pi \pi \ell \bar{\nu}$ (second panel). Replacing the spectator quark, one may obtain the ones for the $B_s \rightarrow K \ell \bar{\nu}$ and $B_s \rightarrow K \pi \ell \bar{\nu}$. The last panel denotes two gluon contributions to $B \rightarrow \pi \pi \ell \bar{\nu}$.

Among all charmless B decays observed so far, the $B \rightarrow \pi \ell \bar{\nu}_\ell$ ($\ell = e, \mu$) has been considered as the most reliable exclusive channel to extract the $|V_{ub}|$. Feynman diagrams for the $B \rightarrow \pi \ell \bar{\nu}$ and $B \rightarrow \pi \pi \ell \bar{\nu}$ (for the convenience of later discussion) are shown in Fig. 5. There is a steady progress in measuring the branching fractions and q^2 -distribution on the experimental side.^{32,33} On the theoretical side, at low q^2 (large recoil) QCD light-cone sum rules (LCSR) is applicable and the leading-twist $\mathcal{O}(\alpha_s^2 \beta_0)$ corrections have been calculated in Ref.³⁴ (see also Ref.^{35,36} for recent LCSR update of $B \rightarrow \pi$ form factors), while the perturbative QCD calculation (pQCD) in k_T factorisation³⁷⁻⁴¹ is rapidly developing.⁴²⁻⁴⁸ At high q^2 (low recoil) region, the Lattice QCD (LQCD) simulation has also achieved great progress.⁴⁹⁻⁵³

For the sake of clarification, let us consider a generic semi-leptonic decay $B \rightarrow P \ell \bar{\nu}_\ell$, where P stands for a light pseudoscalar meson. The transition is induced by the vector current $V^\mu = \bar{u} \gamma^\mu b$ and the hadronic matrix element between the initial and final state can be decomposed as

$$\langle P(p_P) | V^\mu | \bar{B}(p_B) \rangle = F_1(q^2) \left(P^\mu - \frac{m_B^2 - m_P^2}{q^2} q^\mu \right) + F_0(q^2) \frac{m_B^2 - m_P^2}{q^2} q^\mu, \quad (12)$$

where $P^\mu = p_B^\mu + p_P^\mu$. The $F_1(q^2)$ and $F_0(q^2)$ depend only on $q^\mu \equiv p_B^\mu - p_P^\mu$, the momentum transferred to the lepton pair. In the approximation where the leptons are massless, only $F_1(q^2)$ enters the partial decay rate:

$$\frac{d\Gamma(B \rightarrow \pi \ell \bar{\nu}_\ell)}{dq^2} = \frac{G_F^2 |\mathbf{p}_\pi|^3}{24\pi^3} |V_{ub}|^2 |F_1(q^2)|^2, \quad (13)$$

where \mathbf{p}_π is the pion momentum in the B meson rest frame. For the results with massive leptons and various angular distributions, see Ref.⁵⁴

A great advantage in the study of B decays is that the mass m_b of the b -quark is large compared to the QCD hadronic scale Λ and therefore approximations and techniques of heavy quark effective theory can be used. Moreover in the large recoil region, the energy of the π is also large compared to Λ and thus simplifications of

form factors can be achieved in soft-collinear effective theory (SCET).^{55–58} Despite the factorisation property can be proved, non-perturbative theoretical predictions for form factors are usually confined to limited regions of q^2 .

Lattice calculations have been performed in the kinematic region where the outgoing light hadron carries little energy. The first lattice determinations of $F_1(q^2)$ based on unquenched simulations have been obtained by the Fermilab/MILC collaboration⁴⁹ and the HPQCD collaboration,⁵⁰ and they are in substantial agreement. In Ref.,⁴⁹ the b -quark is simulated by using the so-called Fermilab heavy-quark method, while the dependence of the form factor from q^2 is parameterized according to the z -expansion.^{59–61} In Ref.,⁵⁰ the b -quark is simulated by using nonrelativistic QCD and the BK parameterization⁶² is extensively used for the q^2 dependence. Recent results are also available on a fine lattice (lattice spacing $a \sim 0.04$ fm) in the quenched approximations by the QCDSF collaboration.⁵¹ Preliminary results from unquenched Lattice QCD simulation by the FNAL/MILC collaboration can be found in Ref.⁵² Based on the $2 + 1$ flavour domain-wall fermion and Iwasaki gauge-field ensembles generated by the RBC/UKQCD collaboration, Ref.⁵³ has also updated the $B \rightarrow \pi$ form factors.

As a reconciliation of the original QCD sum rule approach^{63,64} and the application of perturbation theory to hard processes, LCSR exhibit several advantages in the calculation of quantities like meson form factors.^{65–69} In the hard scattering region the light-cone operator product expansion (OPE) is applicable, based on which form factors are expressed as a convolution of light-cone distribution amplitudes (LCDA) with a perturbatively calculable hard kernel. Leading twist and a few sub-leading twist LCDA are dominant. Contributions corresponding to higher twist and/or higher multiplicity pion distribution amplitudes are suppressed by powers of $1/m_b$ allowing one to truncate the expansion after a few low twist contributions.

Latest experimental data on $B \rightarrow \pi \ell \bar{\nu}_\ell$ decays come from BaBar³² and Belle.³³ The measured differential decay rates can be fit at low and high q^2 according to LCSR and lattice QCD approaches, respectively. A simultaneous fit to LQCD results has been performed by the two collaborations, which lead to

$$|V_{ub}| = \begin{cases} (3.52 \pm 0.29) \times 10^{-3} & \text{Belle} \\ (3.25 \pm 0.31) \times 10^{-3} & \text{Babar} \end{cases}, \quad (14)$$

where errors are the combined experimental and theoretical uncertainty. Both values are consistent with previous results, but the Belle result has a higher central value by about 1σ .

2.3. Other Semi-Leptonic B decay modes

If the hadronic final state is a vector meson V , both vector and axial currents contribute to the $B \rightarrow V \ell \bar{\nu}_\ell$

$$\langle V(p_V, \epsilon) | V^\mu | \bar{B}(p_B) \rangle = -\frac{2V(q^2)}{m_B + m_V} \epsilon^{\mu\nu\rho\sigma} \epsilon_\nu^* p_{B\rho} p_{V\sigma}, \quad (15)$$

$$\begin{aligned} \langle V(p_V, \epsilon) | A^\mu | \bar{B}(p_B) \rangle &= 2im_V A_0(q^2) \frac{\epsilon^* \cdot q}{q^2} q^\mu + i(m_B + m_V) A_1(q^2) \left[\epsilon_\mu^* - \frac{\epsilon^* \cdot q}{q^2} q^\mu \right] \\ &\quad - iA_2(q^2) \frac{\epsilon^* \cdot q}{m_B + m_V} \left[P^\mu - \frac{m_B^2 - m_V^2}{q^2} q^\mu \right], \end{aligned} \quad (16)$$

where $\varepsilon_{\mu\sigma\nu\rho}$ is the Levi-Civita tensor with the convention $\varepsilon^{0123} = 1$, ϵ^μ is the vector polarization vector and $P = p_B^\mu + p_V^\mu$. Here the momentum transferred to the lepton pair is $q^\mu \equiv p_B^\mu - p_V^\mu$. The differential decay width of $B \rightarrow P_1 P_2 \ell \bar{\nu}_\ell$ including the resonating contribution from $B \rightarrow V \ell \bar{\nu}_\ell$ can be found in Ref.⁵⁴

Recently, BaBar and Belle collaborations have reported significantly improved branching ratios of other heavy-to-light semileptonic decays, that reflects on increased precision for $|V_{ub}|$ values inferred by these decays. These channels include the $B \rightarrow \rho \ell \bar{\nu}_\ell$,³³ $B \rightarrow \omega \ell \bar{\nu}_\ell$ ^{32,33,70} and $B \rightarrow \eta^{(\prime)} \ell \nu_\ell$.³² For the $B \rightarrow \rho$ and $B \rightarrow \omega$ form factors, Belle³³ has used LCSR⁷¹ and LQCD from UKQCD collaboration,⁷² and the extracted $|V_{ub}|$ is in agreement with the ones from $B \rightarrow \pi \ell \bar{\nu}_\ell$. Babar measurement of the $B \rightarrow \omega \ell \bar{\nu}_\ell$ used LCSR form factors⁷¹ and obtained similar values.³² The experimental data on $B \rightarrow \eta^{(\prime)} \ell \bar{\nu}_\ell$ ³² are consistent with theoretical predictions in Refs.,^{73,74} but no result on $|V_{ub}|$ is extracted.

Apart from the observed processes, new channels that are able to extract $|V_{ub}|$ and thus can reduce statistical and systematic uncertainties also deserve theoretical and experimental investigations in future. The $\bar{B}_s^0 \rightarrow K^+ \ell^- \bar{\nu}$ and $\bar{B}_s^0 \rightarrow K^{*+} \ell^- \bar{\nu}$ decays are of this type and have been studied using the state-of-the-art knowledge of form factors in Ref.,⁵⁴ those include not only the recent LQCD calculation⁷⁵ and the LCSR,⁷¹ but also various sets of calculations from the factorisation approach⁴⁷ and QCD-inspired models.⁷⁶⁻⁷⁹

The baryonic $\Lambda_b \rightarrow p$ matrix elements of the vector and axial vector $b \rightarrow u$ currents are parametrized in terms of six independent form factors. At leading-order in $1/m_b$, which becomes exact in the limit $m_b \rightarrow \infty$ and is a good approximation at the physical value of m_b , only two independent form factors remain, and the matrix element with arbitrary Dirac matrix Γ in the current can be written as⁸⁰⁻⁸²

$$\langle p(p', s') | \bar{u} \Gamma b | \Lambda_b(v, s) \rangle = \bar{u}_p(p', s') [F_1 + \not{v} F_2] \Gamma u_{\Lambda_b}(v, s). \quad (17)$$

Here, v is the four-velocity of the Λ_b baryon, and the form factors F_1, F_2 are functions of $p' \cdot v$, the energy of the proton in the Λ_b rest frame. Note that in leading-order SCET, which applies in the limit of large $p' \cdot v$, the form factor F_2 vanishes.⁸³⁻⁸⁵ Calculations of the $\Lambda_b \rightarrow p$ form factors have been performed using light-front quark model,⁸⁶ QCD sum rules^{87,88} and LCSR,⁸⁹⁻⁹² and LQCD.⁹³ We shall wait for the future experimental measurements from LHC and SuperB factories which will make this decay mode also useful to extract the $|V_{ub}|$.

2.4. Purely leptonic decays

In the absence of NP, $B^- \rightarrow \ell^- \bar{\nu}_\ell$ decays are simple tree-level decays, where the two quarks in the initial state, b and \bar{u} , annihilate to a W^- boson. They are particularly

sensitive to physics beyond the SM, since a new particle, for example a charged Higgs boson, may lead the decay taking the place of the W^- boson. In the SM, the $\mathcal{B}(B^- \rightarrow \tau^- \bar{\nu}_\tau)$ is given as

$$\mathcal{B}(B^- \rightarrow \tau^- \bar{\nu}_\tau) = \frac{G_F^2 m_B m_\tau^2}{8\pi} \left(1 - \frac{m_\tau^2}{m_B^2}\right)^2 f_B^2 |V_{ub}|^2 \tau_B, \quad (18)$$

and its measurement can provide a direct experimental determination of the product $f_B |V_{ub}|$. See Ref.⁹⁴ for a recent review on B decays into a τ -lepton.

Experimentally, it is challenging to identify the $B^- \rightarrow \tau^- \bar{\nu}_\tau$ decay because it involves more than one neutrino in the final state and therefore cannot be kinematically constrained. This can be measured in $\Upsilon(4S)$ decays, where one of the B mesons from the $\Upsilon(4S)$ can be tagged in hadronic and semileptonic final states. One then compares properties of the remaining particles to those expected for signal and background. The $B^- \rightarrow \tau^- \bar{\nu}_\tau$ was first observed by Belle in 2006,⁹⁵ and the new average has combined the results from BaBar^{96,97} and Belle:^{98,99}

$$\mathcal{B}(B^- \rightarrow \tau^- \bar{\nu}_\tau) = (1.14 \pm 0.23) \times 10^{-4}. \quad (19)$$

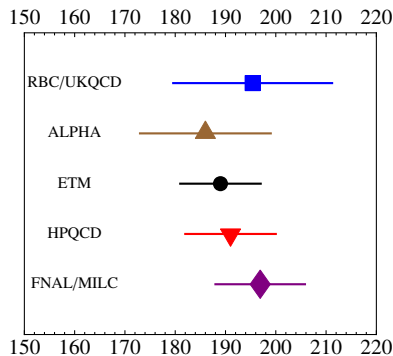


Fig. 6. Decay constant f_B (in units of MeV) from recent Lattice QCD simulations: FNAL/MILC,¹⁰⁰ HPQCD,¹⁰¹ ETM with twisted -mass,¹⁰² ALPHA,¹⁰³ RBC/UKQCD.¹⁰⁴

The extraction of $|V_{ub}|$ relies on the decay constant f_B , and recent LQCD simulations include FNAL/MILC,¹⁰⁰ HPQCD,¹⁰¹ ETM with twisted -mass,¹⁰² ALPHA,¹⁰³ RBC/UKQCD.¹⁰⁴ Based on these results that are collected in Fig. 6 and assuming the errors are independent, we obtain an average

$$f_B = (191.6 \pm 4.4) \text{MeV}, \quad (20)$$

which corresponds to

$$|V_{ub}| = (4.2 \pm 0.4 \pm 0.1) \times 10^{-3}. \quad (21)$$

The first errors come from the $\mathcal{B}(B^- \rightarrow \tau^- \bar{\nu}_\tau)$ as shown in Eq. (19) and the second ones are from f_B . This value seems to be more consistent with the result from the inclusive $b \rightarrow u\ell\bar{\nu}$ decay mode.

It is worthwhile to point out that compared to the averaged branching fraction in Eq. (19), the recent Belle measurement has a lower central value

$$\mathcal{B}(B^- \rightarrow \tau^- \bar{\nu}_\tau) = (0.72_{-0.25}^{+0.27} \pm 0.11) \times 10^{-4}. \quad (22)$$

This corresponds to a smaller $|V_{ub}|$ with a larger uncertainty. Future measurements of $\mathcal{B}(B^- \rightarrow \tau^- \bar{\nu}_\tau)$ will be of great value to make clarifications.

2.5. Theoretical developments on multi-body semileptonic B decays

The $B \rightarrow \rho \ell \bar{\nu}$ and $B_s \rightarrow K^* \ell \bar{\nu}$ reactions receive a complexity due to the large width of ρ (about 150 MeV) and K^* (about 50 MeV). As both ρ and K^* decay into two pseudo-scalars, these processes are quasi-four-body decays, and in principle other resonant and nonresonant states may contribute in the same final state and thereby the $|V_{ub}|$ extraction is contaminated.

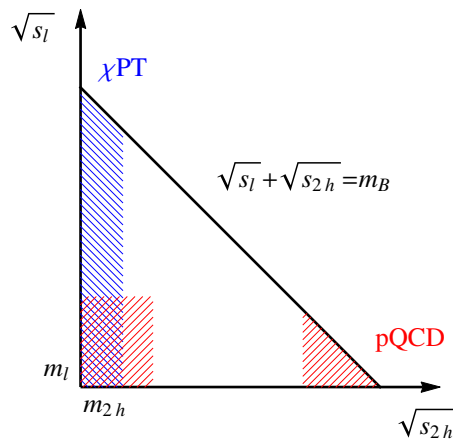


Fig. 7. A sketch of the phase space in the $B \rightarrow P_1 P_2 \ell \bar{\nu}$. $\sqrt{s_l}$ is the lepton pair invariant mass, while $\sqrt{s_{2h}}$ is the invariant mass of the two hadrons. When the two hadrons have a small invariant mass, the interaction is strong and can be described by the chiral perturbation theory. If one or two hadrons in the final state move fast, the hard scattering amplitude can be calculated in QCD.

A general formalism has been developed to incorporate various partial-wave contributions⁵⁴ (similar with the $B \rightarrow K_j^* (\rightarrow K \pi) \ell^+ \ell^-$ case^{105–114} and see also^{115–118}), through which branching fractions, forward-backward asymmetries and polarisations can be projected out. It is worthwhile to stress that the S-wave, whose effects are not negligible, can *not* be expressed in terms of a Breit-Wigner formula, especially for the broad scalar meson $\kappa \equiv K_0^*(800)$ and $\sigma \equiv f_0(600)$. This broad nature is also stressed from the Roy-Steiner representations of the πK scattering.^{119, 120}

The kinematics of the $B \rightarrow P_1 P_2 \ell \bar{\nu}_\ell$ is shown in Fig. 7. In this figure the $\sqrt{s_l}$ is the lepton pair invariant mass, while the $\sqrt{s_{2h}}$ is the invariant mass of the two

hadrons. When the invariant mass of the two hadron is small for instance below 1GeV, chiral perturbation theory (χ PT) is applicable to handle their interactions. When one or two hadrons move fast in the final state, there is a large momentum transfer and thus QCD perturbation theory can be used to calculate the transition.

Using $B \rightarrow K\pi$ as the explicit example, the matrix elements

$$\begin{aligned} \langle (K\pi)_S | \bar{s} \gamma_\mu \gamma_5 b | \bar{B} \rangle &= \frac{-i}{m_{K\pi}} \left\{ \left[P_\mu - \frac{m_B^2 - m_{K\pi}^2}{q^2} q_\mu \right] \mathcal{F}_1^{B \rightarrow K\pi}(m_{K\pi}^2, q^2) \right. \\ &\quad \left. + \frac{m_B^2 - m_{K\pi}^2}{q^2} q_\mu \mathcal{F}_0^{B \rightarrow K\pi}(m_{K\pi}^2, q^2) \right\}, \\ \langle (K\pi)_S | \bar{s} \sigma_{\mu\nu} q^\nu \gamma_5 b | \bar{B} \rangle &= -\frac{\mathcal{F}_T^{B \rightarrow K\pi}(m_{K\pi}^2, q^2)}{m_{K\pi}(m_B + m_{K\pi})} [q^2 P_\mu - (m_B^2 - m_{K\pi}^2) q_\mu], \end{aligned} \quad (23)$$

define the S-wave generalized form factors $\mathcal{F}_i^{54,107,121}$ and project out the S-wave contributions. Here, $P = p_B + p_{K\pi}$ and $q = p_B - p_{K\pi}$.

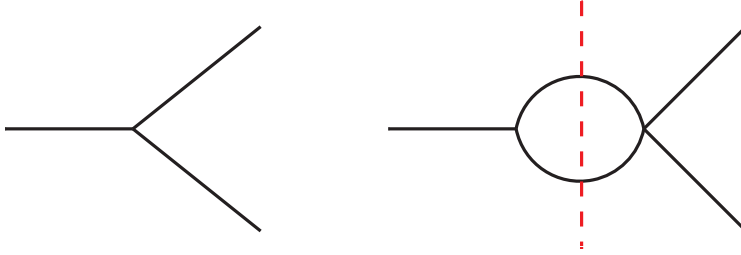


Fig. 8. In the elastic region, the imaginary part (discontinuity) of a form factor (left panel) comes from the one loop diagram shown in the right panel, guaranteed by the Watson's theorem

To avoid the finite-width problem, we will make use of Watson's theorem¹²² which allows a reliable description in terms of scalar form factors. As depicted in Fig. 8, Watson's theorem implies that phases measured in the $K\pi$ elastic scattering and in a decay channel where the $K\pi$ system decouple with other hadrons are equal (modulo π radians). This leads to

$$\langle (K\pi)_S | \bar{s} \Gamma b | \bar{B} \rangle \propto F_{K\pi}(m_{K\pi}^2), \quad (24)$$

where the strangeness-changing scalar $K\pi$ form factors.

The $K\pi$ scattering is strictly elastic below the $K+3\pi$ threshold, about 911 MeV. Inelastic contributions in the $K\pi$ scattering comes from the $K+3\pi$ or $K\eta^{(\prime)}$. In the region from 911 MeV to 1 GeV, the $K+3\pi$ channel has a limited phase space, and thus is generically suppressed. Moreover, as a case-dependent study, it has been demonstrated states with two additional pions will not give sizeable contributions to physical observables.¹²³ The $K\eta^{(\prime)}$ coupled-channel effects can be included in the unitarized approach of χ PT.¹²⁴⁻¹³⁷ We quote recently updated results from Ref.¹⁰⁷

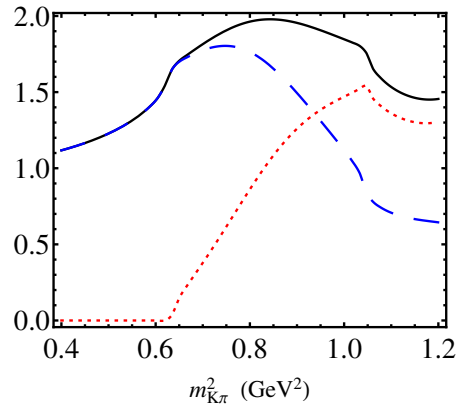


Fig. 9. Scalar $K\pi$ form factors calculated in unitarized χ PT approach. Solid, dashed and dotted lines correspond to the magnitude, the real and imaginary part, in order.

in Fig. 9. Solid, dashed and dotted lines correspond to the magnitude, the real and imaginary part, in order.

For the $\pi\pi$ and $K\bar{K}$ channel, the coupled channel effects should be taken into account, and moreover the standard χ PT may fail to describe the $K\bar{K}$ system as the involved invariant mass is close to 1 GeV. It has been proposed that the unitarized approach which can sum higher order corrections and extend the applicability to energy around 1 GeV. A sketch of the resummation scheme is shown in Fig. 10. Here, T denotes the total scattering amplitude, V is the leading order amplitude and G is the loop integral. For detailed discussions on these form factors, we refer the reader to Ref.^{127,130} The generalisation to the P-wave case is under progress.¹³⁸ Once these quantities are available, they can be used in the study of charmless three-body B decays.^{139–150}

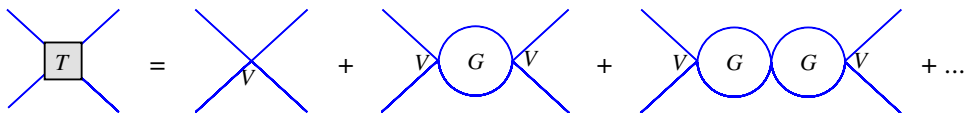


Fig. 10. Sketch of the resummation scheme in the unitarized approach. Here, T denotes the total scattering amplitude, V is the leading order amplitude and G is the loop integral.

In the large recoil region, the $K\pi$ system with invariant mass below 1 GeV moves very fast and therefore can be treated as a light hadron. As shown later this system has similar LCDA with the ones for a light hadron. The transition matrix elements for $B \rightarrow K\pi$ may be factorized in the same way as the ordinary B -to-light ones. At

the leading power, the form factors obey factorization:¹²¹

$$\mathcal{F}_i = C_i \xi(q^2) + \Delta \mathcal{F}_i, \quad (25)$$

where C_i are the short-distance and calculable functions, and ξ is a universal soft form factor derived from the heavy quark $m_b \rightarrow \infty$ and large energy $E \rightarrow \infty$ limit.¹⁵¹ Symmetry breaking terms, starting at order α_s , can be encoded into $\Delta \mathcal{F}_i$, and expressed as a convolution in terms of the LCDA.^{58,152–155}

In Ref.,¹²¹ LCSR has been chosen to calculate the \mathcal{F}_i . The calculation is based on the expansion of the T-product in the correlation function near the light-cone, which produces matrix elements of non-local quark-gluon operators. These quantities are in terms of the generalized LCDA of increasing twist:^{156–159}

$$\langle (K\pi)_S | \bar{s}(x) \Gamma d(0) | 0 \rangle, \quad (26)$$

with Γ being a Dirac matrix. Higher-order calculation will request the gluonic LCDA, whose contribution is shown in Fig. 5. Based on the perturbative calculation in Ref.,^{74,160,161} there is no endpoint singularity and one may directly adopt the collinear factorisation scheme.

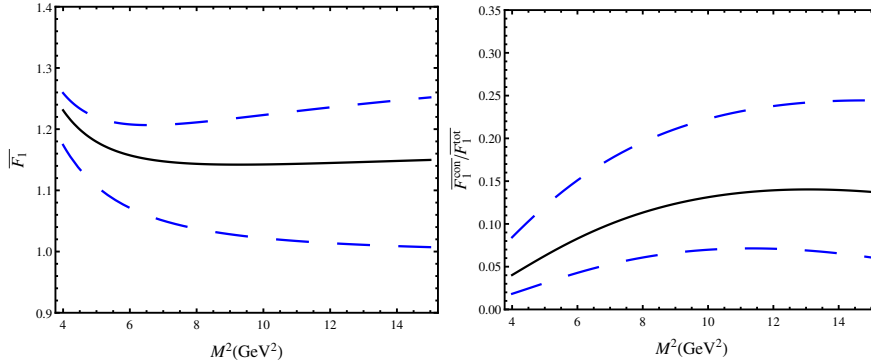


Fig. 11. The dependence of \bar{F}_1 (left panel) and the ratio of continuum and total contributions (right panel) on the Borel parameter. Solid lines denote the central value while dashed curves correspond to variations of threshold parameter: $s_0 = (34 \pm 2)\text{GeV}^2$. Results for \bar{F}_1 are stable when $M^2 > 6 \text{ GeV}^2$, while the continuum contribution is mostly smaller than 30%.

For presentation, one can introduce¹²¹

$$\mathcal{F}_i(q^2, m_{K\pi}^2) = C_X \frac{m_K^2 - m_\pi^2}{m_s - m_u} m_{K\pi} F_{K\pi}(m_{K\pi}^2) \bar{F}_i(m_{K\pi}^2, q^2). \quad (27)$$

The criteria in LCSR to find sets of parameters M^2 (the Borel parameter) and s_0 (the continuum threshold) is that the resulting form factor does not depend much on the precise values of these parameters; additionally both the continuum

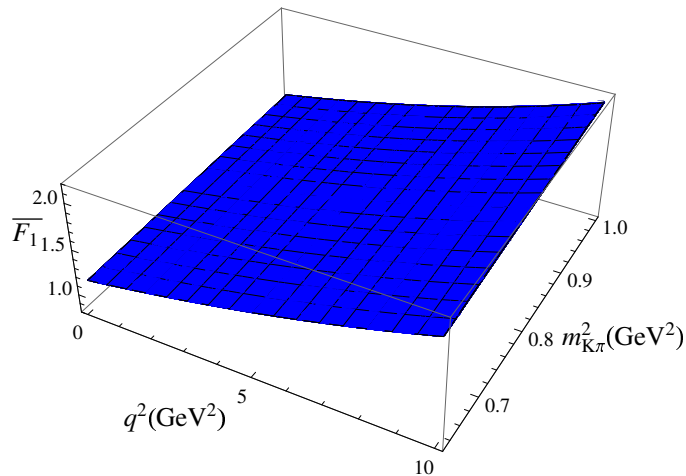


Fig. 12. The dependence of \bar{F}_1 on the squared momentum transfer q^2 and the two-hadron invariant mass square $m_{K\pi}^2$.

contribution and the higher power corrections, arising from the neglected higher twist LCDA, should not be significant. The s_0 is to separate the ground state from higher mass contributions, and thus shall be below the next known resonance, in this case, B_1 with $J^P = 1^+$. Thus approximately this parameter should be close to 33 GeV^2 .⁹ Studies of ordinary heavy-to-light form factors in LCSR, see for instance Ref.,⁷¹ suggested a similar result, ranging from 33 GeV^2 to 36 GeV^2 , while some bigger values are derived in the recent update of $B \rightarrow \pi$ form factor in LCSR.³⁶

Numerical results for the auxiliary function \bar{F}_1 at the $K\pi$ threshold $m_{K\pi} = m_K + m_\pi$ are given in Fig. 11, where the dependence of the form factor \bar{F}_1 (left panel) and the continuum/total ratio (right panel) on the Borel parameter are shown. The continuum contribution to the form factors is obtained by invoking the quark-hadron duality above the threshold s_0 and calculating the correlation function on QCD side. Solid lines denote the central value while dashed curves correspond to variations of threshold parameter: $s_0 = (34 \pm 2)\text{GeV}^2$. From this figure, we can see that results for \bar{F}_1 are stable when $M^2 > 6 \text{ GeV}^2$, and meanwhile the continuum contribution is typically smaller than 30%. Unfortunately, due to the lack of knowledge on the 3-particle twist-3 and higher twist generalized LCDA, their contributions have been neglected.

The dependence on the squared invariant mass of the $K\pi$ system and the squared

momentum transfer q^2 is shown in Fig. 12 with the value $M^2 = 8\text{GeV}^2$.

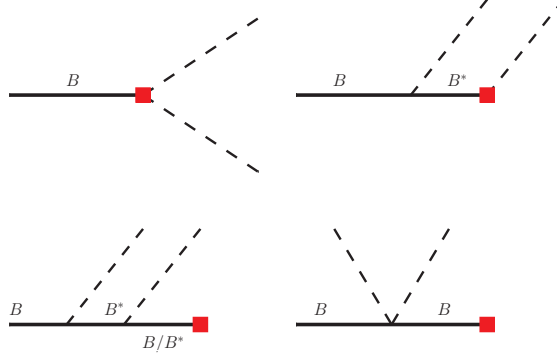


Fig. 13. At the low recoil where all pseudo-Goldstone bosons are having small momentum, the LO Feynman diagrams for the $B \rightarrow \pi\pi\ell\bar{\nu}$ at hadron level are shown. Solid lines and dashed lines represent the heavy mesons and pseudo-Goldstone bosons, respectively. Shaded square denotes an insertion of the weak current.

In Ref.¹⁶² the form factors for the $B \rightarrow \pi\pi$ system are explored in dispersion theory and heavy meson χ PT at low recoil, following the technique employed in Ref.¹¹⁶ At hadron level, Feynman diagrams have been shown in Fig. 13. Solid lines and dashed lines represent heavy mesons and pseudo-Goldstone bosons, respectively. Shaded square denotes an insertion of the weak current. This analysis has taken into account the $\pi - \pi$ rescattering effects, as well as the effect of the ρ meson.

3. γ

β is extracted from the golden mode $B \rightarrow J/\psi K_S$, which is dominated by the $b \rightarrow c\bar{c}s$ transition. Penguin contaminations in this mode are found to be $\mathcal{O}(10^{-3})$ (see Ref.¹⁶³ for a recent discussion). In the case of α , penguins pollutions in $B \rightarrow (\pi, \rho, a_1)\pi$ and $B \rightarrow \rho\rho$ may be sizeable.⁹ The inclusion of isospin related processes, however some of which have small branching ratios, may refine the analysis.

The angle $\gamma \equiv \arg(-V_{ud}V_{ub}^*/(V_{cd}V_{cb}^*))$ is the relative weak phase of decays induced by the $b \rightarrow c\bar{u}s$ and $b \rightarrow u\bar{c}s$ transitions. It can be extracted from tree-dominated modes $B \rightarrow DK$ ^{164–168} whose Feynman diagrams are depicted in Fig. 14. The GLW method^{164,165} uses the fact that the six decay amplitudes of $B^\pm \rightarrow (D^0, \bar{D}^0, D_{CP}^0)K^\pm$ form two triangles in the complex plane, graphically representing

$$\begin{aligned}\sqrt{2}A(B^+ \rightarrow D_\pm^0 K^+) &= A(B^+ \rightarrow D^0 K^+) \pm A(B^+ \rightarrow \bar{D}^0 K^+), \\ \sqrt{2}A(B^- \rightarrow D_\pm^0 K^-) &= A(B^- \rightarrow D^0 K^-) \pm A(B^- \rightarrow \bar{D}^0 K^-),\end{aligned}\quad (28)$$

where the convention $CP|D^0\rangle = |\bar{D}^0\rangle$ has been used and D_\pm^0 (D_\mp^0) is the CP even (odd) eigenstate. Measurements of the six decay rates will fully determine the sides

and apexes of the two triangles, in particular the relative phase between $A(B^- \rightarrow \bar{D}^0 K^-)$ and $A(B^+ \rightarrow D^0 K^+)$ is 2γ .

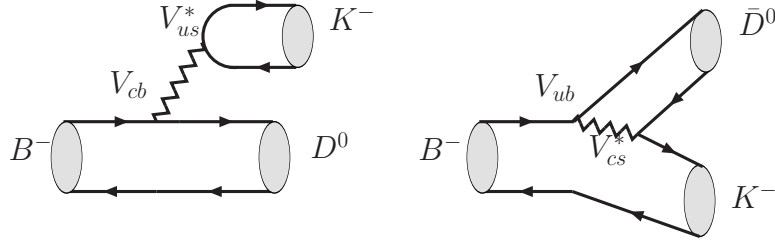


Fig. 14. Feynman diagrams for $B \rightarrow DK$ that can be used to extract the γ angle.

3.1. CP violation effects and errors in $B \rightarrow DK$

Since the identities in Eq. (28) holds irrespective of the strong phase in the decay, this method is free of hadronic uncertainties and is believed theoretically clean. Thus the measurement of γ provides a benchmark of extraction of the CKM parameters.

However the GLW method is based on the neglect of the direct CP asymmetry in D^0 and \bar{D}^0 decays. For instance the $K^+ K^-$ and $\pi^+ \pi^-$ final states can project out the same D_{\pm}^0 . One of the most exciting measurements by LHCb collaboration,¹⁶⁹ confirmed by CDF¹⁷⁰ and Belle¹⁷¹ collaborations, was CP violation in charm sector. These three collaborations have found nonzero difference of CP asymmetries (CPAs) which are much larger than SM expectation. The direct CP violation of D^0 decays was extracted as¹³

$$\Delta A_{CP}^{\text{dir}} = (-0.678 \pm 0.147)\%. \quad (29)$$

However this large value is not confirmed in later analysis by LHCb collaboration¹⁷² and the new average is¹³

$$\Delta A_{CP}^{\text{dir}} = (-0.329 \pm 0.121)\%. \quad (30)$$

Though the new result in Eq. (30) has a smaller central value, the CPA in D decays may play an important role in measuring the γ ^{173–176} (see also Ref.^{177, 178}). Physical observables are given as

$$\begin{aligned} R_+^K &= 2 \frac{\mathcal{B}(B^- \rightarrow D_+^0 K^-) + \mathcal{B}(B^+ \rightarrow D_+^0 K^+)}{\mathcal{B}(B^- \rightarrow D^0 K^-) + \mathcal{B}(B^+ \rightarrow \bar{D}^0 K^+)} \\ &= 1 + (r_B^K)^2 + \frac{2r_B^K \cos \delta_B [(1 + (r_D^f)^2) \cos \gamma + 2r_D^f \cos \delta_D^f]}{1 + (r_D^f)^2 + 2r_D^f \cos \gamma \cos \delta_D^f}, \\ &\equiv 1 + (r_B^K)^2 + 2r_B^K \cos \delta_B^K \cos \gamma_{eff}, \end{aligned} \quad (31)$$

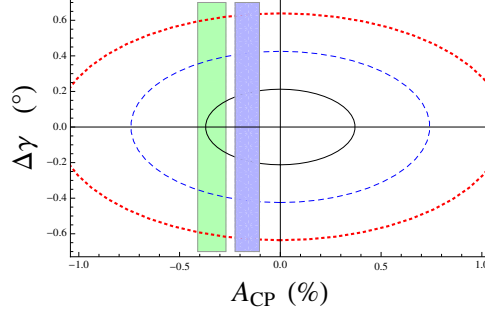


Fig. 15. Effect of CP violation on the extraction of γ via the R_+^K . The sold (black), dashed(blue), and dotted (red) lines correspond to $r_D^f=0.002, 0.004$ and 0.006 respectively. The shadowed region corresponds to $A_{CP}^{K^+K^-} = (-0.34 \pm 0.07)\%$ (left) and $A_{CP}^{K^+K^-} = (-0.16 \pm 0.06)\%$ (right).

$$\begin{aligned}
A_+^K &= \frac{\mathcal{B}(B^- \rightarrow D_+^0 K^-) - \mathcal{B}(B^+ \rightarrow D_+^0 K^+)}{\mathcal{B}(B^- \rightarrow D_+^0 K^-) + \mathcal{B}(B^+ \rightarrow D_+^0 K^+)} \\
&= \frac{1}{R_+^K} \left[(1 - (r_B^K)^2) A_{CP}^{dir}(D^0 \rightarrow f) + \frac{2r_B^K (1 + (r_D^f)^2) \sin \delta_B^K \sin \gamma}{1 + (r_D^f)^2 + 2r_D^f \cos \delta_D^f \cos \gamma} \right] \\
&\equiv 2r_B^K \sin \delta_B^K \sin \gamma_{eff} / R_+^K, \tag{32}
\end{aligned}$$

where the last lines in the above equations correspond to the case with no CPA. r_D^f is the ratio of penguin and tree amplitudes in $D \rightarrow f$ decays, with $f = K^+K^-, \pi^+\pi^-$. γ and δ_D^f is the weak phase difference and strong phase difference respectively. These two equations explicitly show the CPA effects on experimental observables.

The A_+^K in Eq. (32) receives new contributions proportional to the direct CPA in D decays. Neglecting terms suppressed by $\mathcal{O}(r_D^f)$, the dominant correction to $\sin \gamma$ is proportional to $A_{CP}^{dir}(D^0 \rightarrow f)/(2r_B^K \sin \delta_B^K)$. The value for γ obtained from K^+K^- final state and the one from $\pi^+\pi^-$ final states can differ by 3° . Fortunately such effects can be incorporated once the data on the direct CPA is available.

The effects on R_+^K are shown in Fig. 15. The sold (black), dashed(blue), and dotted (red) lines correspond to $r_D^f=0.002, 0.004$ and 0.006 respectively. The shadowed region is the CPA for $D^0 \rightarrow K^+K^-$ from the experimental data: $A_{CP}^{K^+K^-} = (-0.34 \pm 0.07)\%$ (left) and $A_{CP}^{K^+K^-} = (-0.16 \pm 0.06)\%$ (right), where the U-spin symmetry has been assumed for the CP asymmetry $A_{CP}^{K^+K^-} = -A_{CP}^{\pi^+\pi^-} = \Delta A_{CP}/2$.

Recent theoretical works^{179, 180} have investigated other errors to the γ angle and found that these uncertainties are tiny.

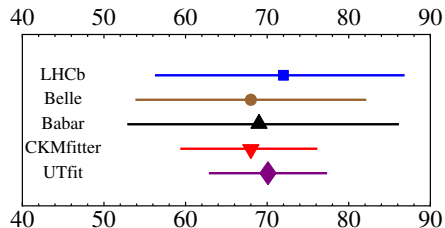


Fig. 16. Recent experimental data on the γ angle vs indirect determination via global fits

3.2. Experimental results

Latest experimental measurements by Belle¹⁸¹ and BaBar¹⁸² collaborations are given as

$$\begin{aligned}\gamma &= (68_{-14}^{+15})^\circ, & \text{Belle} \\ \gamma &= (69_{-16}^{+17})^\circ. & \text{BaBar}\end{aligned}\quad (33)$$

Recently a combination of three LHCb measurements of the CKM angle γ has been presented¹⁸³

$$\gamma = (72.0_{-15.6}^{+14.7})^\circ. \quad \text{LHCb} \quad (34)$$

These results, all of which are consistent with each other, are displayed in Fig. 16, in which we have also shown the global fitting results from CKMfitter¹⁰ and UTfit.¹¹

3.3. B decays into a scalar/tensor state

In the GLW method, the shape of the two triangles formed by decay amplitudes is governed by two quantities

$$\begin{aligned}r_B^K &\equiv |A(B^- \rightarrow \bar{D}^0 K^-)/A(B^- \rightarrow D^0 K^-)|, \\ \delta_B^K &\equiv \arg [e^{i\gamma} A(B^- \rightarrow \bar{D}^0 K^-)/A(B^- \rightarrow D^0 K^-)],\end{aligned}$$

with the world averages from the CKMfitter¹⁰

$$r_B^K = 0.0956_{-0.0064}^{+0.0062}, \quad \delta_B^K = (114.8_{-9.7}^{+9.0})^\circ. \quad (35)$$

The smallness of r_B^K implies the mild sensitivity to γ and thereby the two triangles formed by decay amplitudes are very squashed. $R_{CP^\pm}^K$ and $A_{CP^\pm}^K$ have a mild sensitivity to the angle γ , inducing large experimental uncertainties.

It has been shown in Ref.^{184,185} (see also^{186,187}) that the low sensitivity problem can be highly improved in $B^\pm \rightarrow DK_{0,2}^*$ due to $r_{K_{0,2}^*} \sim 1$, where $K_{0,2}^*$ is a scalar/tensor strange meson. This meson can also be replaced by the $K\pi$ state with the same quantum numbers. Though the color-allowed diagram has a large Wilson coefficient $a_1 \sim 1$, the emitted $K_{0,2}^*$ meson is produced from a local vector or axial-vector current (at the lowest order in α_s), whose matrix element between the QCD vacuum and the $K_0^*(K_2^*)$ state is small (identically zero). Due to this suppression,

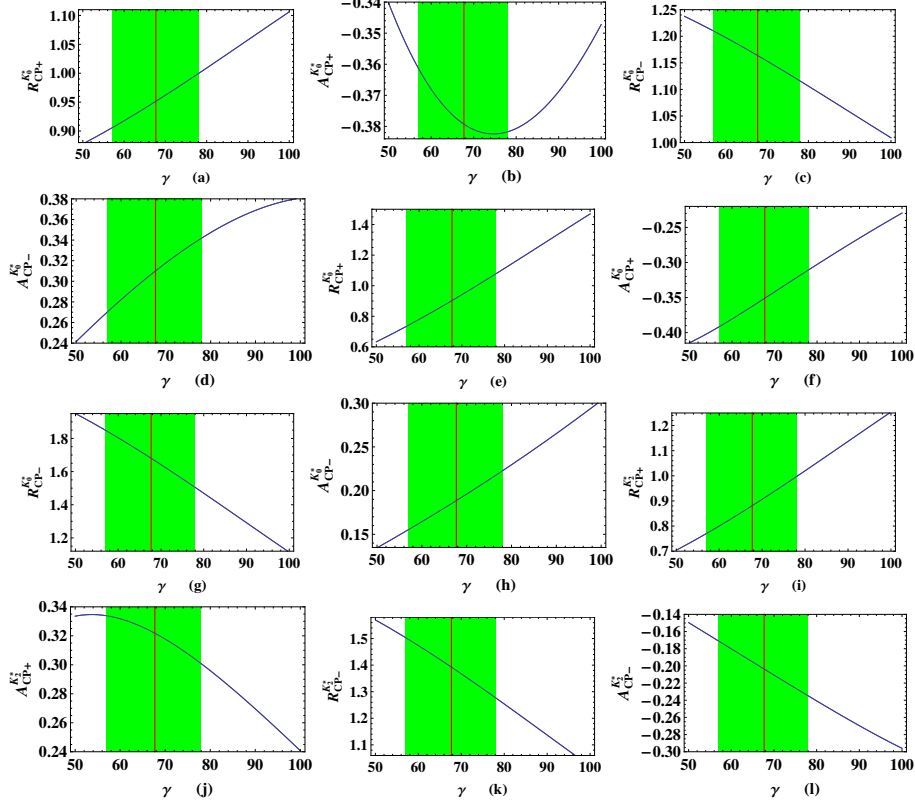


Fig. 17. The dependence of R_{CP} and A_{CP} on γ . Diagrams (a)-(d) show $R_{CP}^{K_0^{*0}}$ and $A_{CP}^{K_0^{*0}}$ in $S1$, (e)-(h) in $S2$, and diagrams (i)-(l) show $R_{CP}^{K_2^{*0}}$ and $A_{CP}^{K_2^{*0}}$. The shadowed (green) region denotes the current bounds on $\gamma = (68_{-11}^{+10})^\circ$ from a combined analysis of $B^\pm \rightarrow DK^\pm$,¹⁰ and the vertical (red) line represents the central value.

the color-allowed amplitude can be comparable to the color-suppressed one. This has been validated by explicit pQCD calculations,^{188–191} using scalar and tensor meson LCDA.^{192–198} Physical observables are defined by:

$$\begin{aligned}
 R_{CP^\pm}^{K_J} &= 2 \frac{\mathcal{B}(B^- \rightarrow D_{CP^\pm} K_J^-) + \mathcal{B}(B^+ \rightarrow D_{CP^\pm} K_J^+)}{\mathcal{B}(B^- \rightarrow D^0 K_J^-) + \mathcal{B}(B^+ \rightarrow \bar{D}^0 K_J^+)} \\
 &= 1 + (r_B^{K_J})^2 \pm 2r_B^{K_J} \cos \delta_B^{K_J} \cos \gamma, \\
 A_{CP^\pm}^{K_J} &= \frac{\mathcal{B}(B^- \rightarrow D_{CP^\pm} K_J^-) - \mathcal{B}(B^+ \rightarrow D_{CP^\pm} K_J^+)}{\mathcal{B}(B^- \rightarrow D_{CP^\pm} K_J^-) + \mathcal{B}(B^+ \rightarrow D_{CP^\pm} K_J^+)} \\
 &= \pm 2r_B^{K_J} \sin \delta_B^{K_J} \sin \gamma / R_{CP^\pm}^{K_J}.
 \end{aligned}$$

The dependence of R_{CP} and A_{CP} on γ is shown in Fig. 17. Diagrams (a)-(d) show $R_{CP}^{K_0^{*0}}$ and $A_{CP}^{K_0^{*0}}$ in first scenario for the structure of scalar mesons, (e)-(h) in second scenario, and diagrams (i)-(l) show $R_{CP}^{K_2^{*0}}$ and $A_{CP}^{K_2^{*0}}$. The shadowed (green)

region denotes the current bounds on $\gamma = (68_{-11}^{+10})^\circ$ from a combined analysis of $B^\pm \rightarrow DK^\pm$,¹⁰ and the vertical (red) line represents the central value.

Properties of useful B decay channels into a scalar/tensor meson towards the extraction of the CKM angle γ are summarised in Tab. 1.

Table 1. Properties of useful B decay channels into a scalar/tensor meson towards the extraction of the CKM angle γ . All these modes are expected to have larger r_f , ratios of decay amplitudes, compared to the corresponding channels in which the scalar/tensor meson is replaced by a pseudo-scalar meson. Branching fractions and ratios of decay amplitudes of $B \rightarrow DT$ are taken from the perturbative QCD calculation¹⁸⁹ while the rest entries when available are obtained in the factorization approximation.¹⁸⁴

Channel	CKM angle to access	BRs for suppressed and allowed modes	r_f
$B^\pm \rightarrow D^\pm K_0^*$	γ	$[4 \times 10^{-6}, 4 \times 10^{-5}]$	0.3
$B^\pm \rightarrow D^\pm K_2^*$	γ	$[3 \times 10^{-6}, 3 \times 10^{-5}]$	0.3
$B \rightarrow D^\pm a_0^\mp$	$\gamma + 2\beta$		0.1
$B \rightarrow D^\pm a_2^\mp$	$\gamma + 2\beta$	$[2 \times 10^{-6}, 4 \times 10^{-4}]$	
$B_s \rightarrow D_s^\pm K_0^{*\mp}$	$\gamma + 2\beta_s$		1
$B_s \rightarrow D_s^\pm K_2^{*\mp}$	$\gamma + 2\beta_s$	$[2 \times 10^{-5}, 2 \times 10^{-5}]$	
$B_s \rightarrow Df_0(980)$	$\gamma + 2\beta_s$	$[1 \times 10^{-6}, 3 \times 10^{-6}]$	0.5
$B_s \rightarrow Df_2'(1525)$	$\gamma + 2\beta_s$	$[3 \times 10^{-6}, 1.4 \times 10^{-5}]$	0.5

3.4. Three-body B decays

It has been proposed in Ref.¹⁹⁹ (see also Ref.^{200,201}) that the $B \rightarrow K\bar{K}K$ and $B \rightarrow K\pi\pi$ can be used to extract the CKM angle γ . These channels are related by the SU(3) symmetry and therefore the extracted result will rely on the symmetry breaking effects.

4. β_s

In the SM, the non-vanishing phase in (bs) triangle is related to the $B_s - \bar{B}_s$ mixing phase. States of B_s^0 or \bar{B}_s^0 at $t = 0$ can evolve in time and thus be mixed with each other. These states at t will be denoted as $B_s(t)$ and $\bar{B}_s(t)$. Since both the B_s^0 and \bar{B}_s^0 can decay into the same final state for instance $J/\psi\phi$, there is an indirect CP asymmetry between the rates of $B_s(t) \rightarrow J/\psi\phi$ and $\bar{B}_s(t) \rightarrow J/\psi\phi$, quantified by

$$\text{Im} \left[\frac{q \bar{A}_f}{p A_f} \right]. \quad (36)$$

Here the A_f and \bar{A}_f are the B_s and \bar{B}_s decay amplitudes which are dominated by the $b \rightarrow c\bar{c}s$ transition. Since the CKM factors $V_{cb}V_{cs}^*$ are real in the standard parametrization of CKM, the indirect CPA defined in Eq. (36) measures the phase of q/p : $\phi_s = -\arg(q/p)$. The ϕ_s is tiny in SM, and in particular $\phi_s = -2\beta_s = -2\arg[-V_{ts}V_{tb}^*/(V_{cs}V_{cb}^*)]$:¹⁷

$$\phi_s = (-0.036 \pm 0.002) \text{ rad.} \quad (37)$$

Any observation of a significant non-zero value would be a NP signal.

The ϕ_s extraction has benefited a lot from the $B_s/\bar{B}_s \rightarrow J/\psi\phi$. Thanks to the large amount of data sample collected by Tevatron and LHC experiments, the result for ϕ_s is getting more and more precise.^{14,202–205} Recently based on the 1.0fb^{-1} data collected at 7 TeV in 2011, the LHCb collaboration gives²⁰⁶

$$\phi_s^{J/\psi\phi} = (0.07 \pm 0.09 \pm 0.01) \text{ rad}, \quad (38)$$

which is in agreement with the SM when errors are taken into account. In addition new alternative channels are proposed and the $B_s \rightarrow J/\psi f_0(980)$ is powerful in reducing the error.^{207,208} Since the $f_0(980)$ is a 0^{++} scalar meson, the final state $J/\psi f_0$ is a CP eigenstate and no angular decomposition is requested. Agreement on branching fractions is found between theoretical calculation^{209–212} and experimental measurements.^{213–215} The ϕ_s is extracted by the LHCb collaboration²⁰⁶

$$\phi_s^{J/\psi f_0} = (-0.14_{-0.16}^{+0.17} \pm 0.01) \text{ rad}. \quad (39)$$

The decay distributions can be derived using helicity amplitudes and for a detailed discussion we refer the reader to Refs.^{216–220} In the presence of S-wave K^+K^- the angular distribution for $B_s \rightarrow J/\psi(\rightarrow l^+l^-)\phi(\rightarrow K^+K^-)$ at the time t of the state that was a pure B_s at $t = 0$ is derived as

$$\frac{d^4\Gamma(t)}{dm_{K\bar{K}}^2 d\cos\theta_K d\cos\theta_l d\phi} = \sum_{k=1}^{10} h_k(t) f_k(\theta_K, \theta_l, \phi), \quad (40)$$

where the time-dependent functions $h_k(t)$ are given as

$$h_k(t) = \frac{3}{4\pi} e^{-\Gamma t} \left\{ a_k \cosh \frac{\Delta\Gamma t}{2} + b_k \sinh \frac{\Delta\Gamma t}{2} + c_k \cos(\Delta m t) + d_k \sin(\Delta m t) \right\} \quad (41)$$

Here $\Delta m = m_H - m_L$, $\Delta\Gamma = \Gamma_L - \Gamma_H$, and $\Gamma = (\Gamma_L + \Gamma_H)/2$. For the state that was a \bar{B}_s at $t = 0$, the signs in front of c_k and d_k should be reversed. Explicit results for these coefficients are given for instance in Ref.²²⁰

On the theoretical side, although decays of the B_s/B_s^0 meson into $J/\psi(\phi/f_0)$ are mainly governed by the $b \rightarrow c\bar{c}s$ transition at the quark level, there are penguin contributions with non-vanishing different weak phases. Thus the indirect CPA can be moved away from the ϕ_s . Intuitively penguin contribution is expected to be small in the SM, but a complete and reliable estimate of its effects by some QCD-inspired approach is requested. Such estimate will become mandatory soon. As a reference, after the upgrade of LHC the error can be diminished to $\Delta\phi_s \sim 0.008$.¹⁴

Ref.²²⁰ has attempted to estimate the penguin contributions in the $B \rightarrow J/\psi V$ decays and explore the impact to the CPA measurement, following the calculation in Ref.^{163,221–223} Instead of using the flavor SU(3) symmetry to relate the effects in $B_s \rightarrow J/\psi\phi$ and the counterpart of B decay modes,^{224,225} the pQCD approach has been used to directly compute both tree amplitudes and penguin amplitudes. Apart from LO contributions, NLO order corrections in α_s have been included, which are sizeable especially to penguin contributions.

The mixing phase is given as

$$\phi_s^{\text{eff}} = -\arg \left[\frac{q}{p} \frac{\bar{\mathcal{A}}_f^\alpha}{\mathcal{A}_f^\alpha} \right] = \phi_s + \Delta\phi_s, \quad (42)$$

where α denotes three polarization configurations L , \parallel , and \perp , and $\mathcal{A}_f^\alpha(\bar{\mathcal{A}}_f^\alpha)$ stands for the decay amplitude of $B_s \rightarrow J/\psi\phi$ ($\bar{B}_s \rightarrow J/\psi\phi$), which can be decomposed into²²⁵

$$\mathcal{A}_f^\alpha(B_s \rightarrow J/\psi\phi) = V_{cb}^* V_{cs}(T_c^\alpha + P_c^\alpha + P_t^\alpha) + V_{ub}^* V_{us}(P_u^\alpha + P_t^\alpha). \quad (43)$$

Here, the unitarity relation $V_{tb}^* V_{ts} = -V_{cb}^* V_{cs} - V_{ub}^* V_{us}$ for the CKM matrix elements has been used. The tree amplitude T_c^α is dominant to $\mathcal{B}(B_s \rightarrow J/\psi\phi)$, while P_c^α , P_u^α , and P_t^α are penguin pollutions. The u-quark and c-quark penguin were not included in Ref.²²⁰ Then the charge conjugation amplitude for $B_s \rightarrow J/\psi\phi$ decay is

$$\bar{\mathcal{A}}_f^\alpha(\bar{B}_s \rightarrow J/\psi\phi) = V_{cb}^* V_{cs}(T_c^\alpha + P_c^\alpha + P_t^\alpha) + V_{ub}^* V_{us}(P_u^\alpha + P_t^\alpha). \quad (44)$$

For simplicity, one can introduce the ratio

$$a_f e^{i\delta_f + i\gamma} \equiv \frac{V_{ub}^* V_{us}(P_u^\alpha + P_t^\alpha)}{V_{cb}^* V_{cs}(T_c^\alpha + P_c^\alpha + P_t^\alpha)}, \quad (45)$$

which leads to

$$\frac{\bar{\mathcal{A}}_f^\alpha}{\mathcal{A}_f^\alpha} = \frac{1 + a_f e^{i\delta_f - i\gamma}}{1 + a_f e^{i\delta_f + i\gamma}} \simeq 1 - 2ia_f \cos \delta_f \sin \gamma, \quad (46)$$

and the phase shift:

$$\Delta\phi_s \simeq \arcsin(2a_f \cos \delta_f \sin \gamma). \quad (47)$$

With the inclusion of various parametric errors, the quantity $\Delta\phi_s$ from the pQCD calculation is predicted as follows²²⁰

$$\begin{aligned} \Delta\phi_s(L) &\approx 0.96_{-0.03}^{+0.04}(\omega_B)_{-0.00}^{+0.02}(f_M)_{-0.01}^{+0.01}(a_i)_{-0.02}^{+0.03}(m_c) [0.96_{-0.04}^{+0.05}] \times 10^{-3}; \\ \Delta\phi_s(\parallel) &\approx 0.84_{-0.02}^{+0.02}(\omega_B)_{-0.00}^{+0.00}(f_M)_{-0.01}^{+0.01}(a_i)_{-0.01}^{+0.00}(m_c) [0.84_{-0.02}^{+0.02}] \times 10^{-3}; \\ \Delta\phi_s(\perp) &\approx 0.80_{-0.01}^{+0.01}(\omega_B)_{-0.00}^{+0.00}(f_M)_{-0.01}^{+0.01}(a_i)_{-0.02}^{+0.00}(m_c) [0.80_{-0.02}^{+0.01}] \times 10^{-3}. \end{aligned} \quad (48)$$

The values as given in the parentheses have been added in quadrature.

Thanks to the large amount of data sample, the LHCb experiment is able to perform an analysis of the angular distribution of $B_s \rightarrow J/\psi\phi$. Predictions for the P-wave coefficients (in units of 10^{-3}) are as follows:

f_k	Δa_k	Δb_k	Δc_k	Δd_k
$c_K^2 s_l^2$	0.28	0.32	-0.3	1.0
$\frac{s_K^2(1-c_\phi^2 c_l^2)}{2}$	-0.83	1.52	0.84	-1.0
$\frac{s_K^2(1-s_\phi^2 c_l^2)}{2}$	-1.1	-1.8	1.2	1.1
$s_K^2 s_l^2 s_\phi c_\phi$	-0.1	1.1	6.4	1.0
$\sqrt{2} s_K c_K s_l c_l c_\phi$	-1.0	1.0	0.3	0.03
$\sqrt{2} s_K c_K s_l c_l s_\phi$	1.1	-0.02	-44	-1.4

Most of the results for the other coefficients are of order 10^{-3} . The other four angular coefficients are the S-wave and the interference terms. The study of them requests the calculation of $B_s \rightarrow J/\psi(K^+K^-)_S$, presumably dominated by the $f_0(980)$.

Though these results should be taken with caution as only part of the known NLO contributions is included, the deviation is found to be of $\mathcal{O}(10^{-3})$, and it may provide an important SM reference for verifying the existing NP from the $B_s \rightarrow J/\psi\phi$ data.

5. Summary and Outlook

Up to this date, the CKM mechanism continues to give a consistent explanation of most available data on the flavor observables and CP violation with an incredible accuracy. This great success, together with the observation of Higgs boson consistent with the SM,^{226,227} implies that the NP effects should be tiny and renders the precision predictions for the involved quantities particularly important.

Despite the success, there are still unsatisfactory in this mechanism and thus perhaps some room for NP. In this review, we have focused on the heavy flavour sector and have discussed three quantities of the CKM matrix in order to give an idea of the current status of the field. These quantities are quite uncertain at this stage.

- The $|V_{ub}|$ can be extracted from inclusive and exclusive semileptonic B decays. Deviations are found in the two determinations but the significance, at about 3σ level, is still low.
- The angle γ has the largest error, about 10° , compared to the other two CKM angles α, β . This is the main source of errors in the unitarity triangle and currently does not allow us for a direct test of CKM unitarity.
- The $B_s - \bar{B}_s$ mixing phase is predicted tiny in the SM. The current experimental results are extracted from $B_s \rightarrow J/\psi\phi$ and $B_s \rightarrow J/\psi f_0(980)$.

Improving the knowledge on the CKM renders the precise theoretical predictions and experimental measurements important. The reduction of experimental uncertainties seems to have a promising prospect in near future, due to the large amount of data sample (to be) collected at LHC¹⁴ and the forthcoming Super KEKB factory.¹⁶ So we are heading towards exciting times in CKM and flavour physics.

Acknowledgments

The author is very grateful to Yu-Ming Wang and Yue-Hong Xie for useful discussions, collaborations and carefully reading the manuscript. He also thanks Hai-Yang Cheng, Feng-Kun Guo, Christoph Hanhart, Bastian Kubis, Gang Li, Hsiang-Nan Li, Run-Hui Li, Ying Li, Xin Liu, Cai-Dian Lü, Ulf-G. Meißner, Qin Qin, Yue-Long Shen, Wen-Fei Wang, Fu-Sheng Yu, Zhi-Qing Zhang, and Zhi-Tian Zou for useful discussions. This work is supported in part by the DFG and the NSFC through

funds provided to the Sino-German CRC 110 “Symmetries and the Emergence of Structure in QCD”.

References

1. N. Cabibbo, Phys. Rev. Lett. **10**, 531 (1963).
2. M. Kobayashi and T. Maskawa, Prog. Theor. Phys. **49**, 652 (1973).
3. L. Wolfenstein, Phys. Rev. Lett. **51**, 1945 (1983).
4. Y. H. Ahn, H. -Y. Cheng and S. Oh, Phys. Lett. B **703**, 571 (2011) [arXiv:1106.0935 [hep-ph]].
5. G. Ricciardi, Mod. Phys. Lett. A **28**, 1330016 (2013) [arXiv:1305.2844 [hep-ph]].
6. G. Ricciardi, arXiv:1403.7750 [hep-ph].
7. Z. -J. Xiao, Y. -Y. Fan, W. -F. Wang and S. Cheng, arXiv:1401.0571 [hep-ph].
8. A. Lenz, arXiv:1404.6197 [hep-ph].
9. J. Beringer *et al.* [Particle Data Group Collaboration], Phys. Rev. D **86**, 010001 (2012).
10. J. Charles *et al.* [CKMfitter Group Collaboration], Eur. Phys. J. C **41**, 1 (2005) [hep-ph/0406184], updated results and plots available at: <http://ckmfitter.in2p3.fr>.
11. M. Ciuchini *et al.* [UTfit Group Collaboration], JHEP **0107**, 013 (2001) [hep-ph/0012308], updated results and plots available at: <http://www.utfit.org/UTfit/WebHome>.
12. G. Eigen, G. Dubois-Felsmann, D. G. Hitlin and F. C. Porter, Phys. Rev. D **89**, 033004 (2014) [arXiv:1301.5867 [hep-ex]].
13. Y. Amhis *et al.* [Heavy Flavor Averaging Group Collaboration], arXiv:1207.1158 [hep-ex].
14. R. Aaij *et al.* [LHCb Collaboration], Eur. Phys. J. C **73**, 2373 (2013) [arXiv:1208.3355 [hep-ex]].
15. M. Bona *et al.* [SuperB Collaboration], Pisa, Italy: INFN (2007) 453 p. www.pi.infn.it/SuperB/?q=CDR [arXiv:0709.0451 [hep-ex]].
16. T. Aushev, W. Bartel, A. Bondar, J. Brodzicka, T. E. Browder, P. Chang, Y. Chao and K. F. Chen *et al.*, arXiv:1002.5012 [hep-ex].
17. J. Charles, O. Deschamps, S. Descotes-Genon, R. Itoh, H. Lacker, A. Menzel, S. Monteil and V. Niess *et al.*, Phys. Rev. D **84**, 033005 (2011) [arXiv:1106.4041 [hep-ph]].
18. T. Aaltonen *et al.* [CDF Collaboration], Phys. Rev. Lett. **100**, 161802 (2008) [arXiv:0712.2397 [hep-ex]].
19. V. M. Abazov *et al.* [D0 Collaboration], Phys. Rev. Lett. **101**, 241801 (2008) [arXiv:0802.2255 [hep-ex]].
20. C. S. Kim and Y. Li, Eur. Phys. J. C **71**, 1531 (2011) [arXiv:1007.2291 [hep-ph]].
21. A. Crivellin and S. Pokorski, arXiv:1407.1320 [hep-ph].
22. M. Brucherseifer, F. Caola and K. Melnikov, Phys. Lett. B **721**, 107 (2013) [arXiv:1302.0444 [hep-ph]].
23. B. O. Lange, M. Neubert and G. Paz, Phys. Rev. D **72**, 073006 (2005) [hep-ph/0504071].
24. S. W. Bosch, B. O. Lange, M. Neubert and G. Paz, Nucl. Phys. B **699**, 335 (2004) [hep-ph/0402094].
25. P. Gambino, P. Giordano, G. Ossola and N. Uraltsev, JHEP **0710**, 058 (2007) [arXiv:0707.2493 [hep-ph]].
26. J. R. Andersen and E. Gardi, JHEP **0601**, 097 (2006) [hep-ph/0509360].
27. U. Aglietti and G. Ricciardi, Phys. Rev. D **70**, 114008 (2004) [hep-ph/0407225].
28. U. Aglietti, G. Ferrera and G. Ricciardi, Nucl. Phys. B **768**, 85 (2007) [hep-

- ph/0608047].
29. U. Aglietti, F. Di Lodovico, G. Ferrera and G. Ricciardi, *Eur. Phys. J. C* **59**, 831 (2009) [arXiv:0711.0860 [hep-ph]].
 30. P. Urquijo *et al.* [Belle Collaboration], *Phys. Rev. Lett.* **104**, 021801 (2010) [arXiv:0907.0379 [hep-ex]].
 31. J. P. Lees *et al.* [BaBar Collaboration], *Phys. Rev. D* **86**, 032004 (2012) [arXiv:1112.0702 [hep-ex]].
 32. J. P. Lees *et al.* [BaBar Collaboration], *Phys. Rev. D* **86**, 092004 (2012) [arXiv:1208.1253 [hep-ex]].
 33. A. Sibidanov *et al.* [Belle Collaboration], *Phys. Rev. D* **88**, no. 3, 032005 (2013) [arXiv:1306.2781 [hep-ex]].
 34. A. Bharucha, *JHEP* **1205**, 092 (2012) [arXiv:1203.1359 [hep-ph]].
 35. Z. -H. Li, N. Zhu, X. -J. Fan and T. Huang, *JHEP* **1205**, 160 (2012) [arXiv:1206.0091 [hep-ph]].
 36. A. Khodjamirian, T. Mannel, N. Offen and Y. -M. Wang, *Phys. Rev. D* **83**, 094031 (2011) [arXiv:1103.2655 [hep-ph]].
 37. Y. -Y. Keum, H. -n. Li and A. I. Sanda, *Phys. Lett. B* **504**, 6 (2001) [hep-ph/0004004].
 38. Y. Y. Keum, H. -N. Li and A. I. Sanda, *Phys. Rev. D* **63**, 054008 (2001) [hep-ph/0004173].
 39. C. -D. Lu, K. Ukai and M. -Z. Yang, *Phys. Rev. D* **63**, 074009 (2001) [hep-ph/0004213].
 40. C. -D. Lu and M. -Z. Yang, *Eur. Phys. J. C* **23**, 275 (2002) [hep-ph/0011238].
 41. T. Kurimoto, H. -n. Li and A. I. Sanda, *Phys. Rev. D* **65**, 014007 (2002) [hep-ph/0105003].
 42. H. -n. Li, Y. -L. Shen, Y. -M. Wang and H. Zou, *Phys. Rev. D* **83**, 054029 (2011) [arXiv:1012.4098 [hep-ph]].
 43. H. -n. Li, Y. -L. Shen and Y. -M. Wang, *Phys. Rev. D* **85**, 074004 (2012) [arXiv:1201.5066 [hep-ph]].
 44. H. -C. Hu and H. -n. Li, *Phys. Lett. B* **718**, 1351 (2013) [arXiv:1204.6708 [hep-ph]].
 45. H. -N. Li, Y. -L. Shen and Y. -M. Wang, *JHEP* **1302**, 008 (2013) [arXiv:1210.2978 [hep-ph]].
 46. H. -N. Li, Y. -L. Shen and Y. -M. Wang, *JHEP* **1401**, 004 (2014) [arXiv:1310.3672 [hep-ph]].
 47. W. -F. Wang and Z. -J. Xiao, *Phys. Rev. D* **86**, 114025 (2012) [arXiv:1207.0265 [hep-ph]].
 48. S. Cheng, Y. -Y. Fan, X. Yu, C. -D. Lü and Z. -J. Xiao, arXiv:1402.5501 [hep-ph].
 49. J. A. Bailey, C. Bernard, C. E. DeTar, M. Di Pierro, A. X. El-Khadra, R. T. Evans, E. D. Freeland and E. Gamiz *et al.*, *Phys. Rev. D* **79**, 054507 (2009) [arXiv:0811.3640 [hep-lat]].
 50. E. Dalgic, A. Gray, M. Wingate, C. T. H. Davies, G. P. Lepage and J. Shigemitsu, *Phys. Rev. D* **73**, 074502 (2006) [Erratum-ibid. *D* **75**, 119906 (2007)] [hep-lat/0601021].
 51. A. Al-Haydari *et al.* [QCDSF Collaboration], *Eur. Phys. J. A* **43**, 107 (2010) [arXiv:0903.1664 [hep-lat]].
 52. D. Du, J. A. Bailey, A. Bazavov, C. Bernard, A. X. El-Khadra, S. Gottlieb, R. D. Jain and A. S. Kronfeld *et al.*, *PoS LATTICE* **2013**, 383 (2013) [arXiv:1311.6552 [hep-lat]].
 53. T. Kawanai, R. S. Van de Water and O. Witzel, arXiv:1311.1143 [hep-lat].
 54. U. -G. Meißner and W. Wang, *JHEP* **1401**, 107 (2014) [arXiv:1311.5420 [hep-ph]].
 55. C. W. Bauer, S. Fleming and M. E. Luke, *Phys. Rev. D* **63**, 014006 (2000) [hep-

- ph/0005275].
56. C. W. Bauer, S. Fleming, D. Pirjol and I. W. Stewart, Phys. Rev. D **63**, 114020 (2001) [hep-ph/0011336].
 57. C. W. Bauer, D. Pirjol and I. W. Stewart, Phys. Rev. D **65**, 054022 (2002) [hep-ph/0109045].
 58. M. Beneke and T. Feldmann, Nucl. Phys. B **685**, 249 (2004) [hep-ph/0311335].
 59. T. Becher and R. J. Hill, Phys. Lett. B **633**, 61 (2006) [hep-ph/0509090].
 60. M. C. Arnesen, B. Grinstein, I. Z. Rothstein and I. W. Stewart, Phys. Rev. Lett. **95**, 071802 (2005) [hep-ph/0504209].
 61. C. Bourrely, I. Caprini and L. Lellouch, Phys. Rev. D **79**, 013008 (2009) [Erratum-ibid. D **82**, 099902 (2010)] [arXiv:0807.2722 [hep-ph]].
 62. D. Becirevic and A. B. Kaidalov, Phys. Lett. B **478**, 417 (2000) [hep-ph/9904490].
 63. M. A. Shifman, A. I. Vainshtein and V. I. Zakharov, Nucl. Phys. B **147**, 385 (1979).
 64. M. A. Shifman, A. I. Vainshtein and V. I. Zakharov, Nucl. Phys. B **147**, 448 (1979).
 65. N. S. Craigie and J. Stern, Nucl. Phys. B **216**, 209 (1983).
 66. V. M. Braun and I. E. Filyanov, Z. Phys. C **44**, 157 (1989) [Sov. J. Nucl. Phys. **50**, 511 (1989)] [Yad. Fiz. **50**, 818 (1989)].
 67. V. L. Chernyak and I. R. Zhitnitsky, Nucl. Phys. B **345**, 137 (1990).
 68. V. M. Belyaev, V. M. Braun, A. Khodjamirian and R. Ruckl, Phys. Rev. D **51**, 6177 (1995) [hep-ph/9410280].
 69. P. Colangelo and A. Khodjamirian, In *Shifman, M. (ed.): At the frontier of particle physics, vol. 3* 1495-1576 [hep-ph/0010175].
 70. J. P. Lees *et al.* [BaBar Collaboration], Phys. Rev. D **88**, 072006 (2013) [arXiv:1308.2589 [hep-ex]].
 71. P. Ball and R. Zwicky, Phys. Rev. D **71**, 014029 (2005) [hep-ph/0412079].
 72. L. Del Debbio *et al.* [UKQCD Collaboration], Phys. Lett. B **416**, 392 (1998) [hep-lat/9708008].
 73. C. -H. Chen, Y. -L. Shen and W. Wang, Phys. Lett. B **686**, 118 (2010) [arXiv:0911.2875 [hep-ph]].
 74. W. -F. Wang, Y. -Y. Fan, M. Liu and Z. -J. Xiao, Phys. Rev. D **87**, 097501 (2013) [arXiv:1301.0197].
 75. R. R. Horgan, Z. Liu, S. Meinel and M. Wingate, arXiv:1310.3722 [hep-lat].
 76. R. N. Faustov and V. O. Galkin, Phys. Rev. D **87**, no. 9, 094028 (2013) [arXiv:1304.3255].
 77. H. -Y. Cheng, C. -K. Chua and C. -W. Hwang, Phys. Rev. D **69**, 074025 (2004) [hep-ph/0310359].
 78. C. -D. Lu, W. Wang and Z. -T. Wei, Phys. Rev. D **76**, 014013 (2007) [hep-ph/0701265 [HEP-PH]].
 79. R. C. Verma, J. Phys. G **39**, 025005 (2012) [arXiv:1103.2973 [hep-ph]].
 80. F. Hussain, D. -S. Liu, M. Kramer, J. G. Korner and S. Tawfiq, Nucl. Phys. B **370**, 259 (1992).
 81. T. Mannel, W. Roberts and Z. Ryzak, Nucl. Phys. B **355**, 38 (1991).
 82. F. Hussain, J. G. Korner, M. Kramer and G. Thompson, Z. Phys. C **51**, 321 (1991).
 83. T. Feldmann and M. W. Y. Yip, Phys. Rev. D **85**, 014035 (2012) [Erratum-ibid. D **86**, 079901 (2012)] [arXiv:1111.1844 [hep-ph]].
 84. T. Mannel and Y. -M. Wang, JHEP **1112**, 067 (2011) [arXiv:1111.1849 [hep-ph]].
 85. W. Wang, Phys. Lett. B **708**, 119 (2012) [arXiv:1112.0237 [hep-ph]].
 86. Z. -T. Wei, H. -W. Ke and X. -Q. Li, Phys. Rev. D **80**, 094016 (2009) [arXiv:0909.0100 [hep-ph]].
 87. C. -S. Huang, C. -F. Qiao and H. -G. Yan, Phys. Lett. B **437**, 403 (1998) [hep-

- ph/9805452].
88. R. S. Marques de Carvalho, F. S. Navarra, M. Nielsen, E. Ferreira and H. G. Dosch, Phys. Rev. D **60**, 034009 (1999) [hep-ph/9903326].
 89. M. -q. Huang and D. -W. Wang, Phys. Rev. D **69**, 094003 (2004) [hep-ph/0401094].
 90. Y. -M. Wang, Y. -L. Shen and C. -D. Lu, Phys. Rev. D **80**, 074012 (2009) [arXiv:0907.4008 [hep-ph]].
 91. K. Azizi, M. Bayar, Y. Sarac and H. Sundu, Phys. Rev. D **80**, 096007 (2009) [arXiv:0908.1758 [hep-ph]].
 92. A. Khodjamirian, C. Klein, T. Mannel and Y. -M. Wang, JHEP **1109**, 106 (2011) [arXiv:1108.2971 [hep-ph]].
 93. W. Detmold, C. -J. D. Lin, S. Meinel and M. Wingate, Phys. Rev. D **88**, 014512 (2013) [arXiv:1306.0446 [hep-lat]].
 94. A. Soffer, Mod. Phys. Lett. A **29**, no. 7, 1430007 (2014) [arXiv:1401.7947 [hep-ex]].
 95. K. Ikado *et al.* [Belle Collaboration], Phys. Rev. Lett. **97**, 251802 (2006) [hep-ex/0604018].
 96. B. Aubert *et al.* [BaBar Collaboration], Phys. Rev. D **81**, 051101 (2010) [arXiv:0912.2453 [hep-ex]].
 97. J. P. Lees *et al.* [BaBar Collaboration], Phys. Rev. D **88**, no. 3, 031102 (2013) [arXiv:1207.0698 [hep-ex]].
 98. K. Hara *et al.* [Belle Collaboration], Phys. Rev. D **82**, 071101 (2010) [arXiv:1006.4201 [hep-ex]].
 99. I. Adachi *et al.* [Belle Collaboration], Phys. Rev. Lett. **110**, 131801 (2013) [arXiv:1208.4678 [hep-ex]].
 100. A. Bazavov *et al.* [Fermilab Lattice and MILC Collaborations], Phys. Rev. D **85**, 114506 (2012) [arXiv:1112.3051 [hep-lat]].
 101. H. Na, C. J. Monahan, C. T. H. Davies, R. Horgan, G. P. Lepage and J. Shigemitsu, Phys. Rev. D **86**, 034506 (2012) [arXiv:1202.4914 [hep-lat]].
 102. N. Carrasco *et al.* [ETM Collaboration], JHEP **1403**, 016 (2014) [arXiv:1308.1851 [hep-lat]].
 103. F. Bernardoni, B. Blossier, J. Bulava, M. Della Morte, P. Fritzsche, N. Garron, A. Gerardin and J. Heitger *et al.*, arXiv:1404.3590 [hep-lat].
 104. N. H. Christ, J. M. Flynn, T. Izubuchi, T. Kawanai, C. Lehner, A. Soni, R. S. Van de Water and O. Witzel, arXiv:1404.4670 [hep-lat].
 105. F. Kruger, L. M. Sehgal, N. Sinha and R. Sinha, Phys. Rev. D **61**, 114028 (2000) [Erratum-ibid. D **63**, 019901 (2001)] [hep-ph/9907386].
 106. C. -D. Lu and W. Wang, Phys. Rev. D **85**, 034014 (2012) [arXiv:1111.1513 [hep-ph]].
 107. M. Doring, U. -G. Meißner and W. Wang, JHEP **1310**, 011 (2013) [arXiv:1307.0947 [hep-ph]].
 108. R. -H. Li, C. -D. Lu and W. Wang, Phys. Rev. D **83**, 034034 (2011) [arXiv:1012.2129 [hep-ph]].
 109. D. Becirevic and A. Tayduganov, Nucl. Phys. B **868**, 368 (2013) [arXiv:1207.4004 [hep-ph]].
 110. J. Matias, Phys. Rev. D **86**, 094024 (2012) [arXiv:1209.1525 [hep-ph]].
 111. T. Blake, U. Egede and A. Shires, JHEP **1303**, 027 (2013) [arXiv:1210.5279 [hep-ph]].
 112. C. Bobeth, G. Hiller and D. van Dyk, Phys. Rev. D **87**, 034016 (2013) [arXiv:1212.2321 [hep-ph]].
 113. S. Descotes-Genon, T. Hurth, J. Matias and J. Virto, JHEP **1305**, 137 (2013) [arXiv:1303.5794 [hep-ph]].
 114. S. Descotes-Genon, J. Matias and J. Virto, Phys. Rev. D **88**, 074002 (2013) [arXiv:1307.5683 [hep-ph]].

115. G. Kopp, G. Kramer, G. A. Schuler and W. F. Palmer, *Z. Phys. C* **48**, 327 (1990).
116. C. L. Y. Lee, M. Lu and M. B. Wise, *Phys. Rev. D* **46**, 5040 (1992).
117. B. Ananthanarayan and K. Shivaraj, *Phys. Lett. B* **628**, 223 (2005) [hep-ph/0508116].
118. S. Faller, T. Feldmann, A. Khodjamirian, T. Mannel and D. van Dyk, *Phys. Rev. D* **89**, 014015 (2014) [arXiv:1310.6660 [hep-ph]].
119. P. Buettiker, S. Descotes-Genon and B. Moussallam, *Eur. Phys. J. C* **33**, 409 (2004) [hep-ph/0310283].
120. S. Descotes-Genon and B. Moussallam, *Eur. Phys. J. C* **48**, 553 (2006) [hep-ph/0607133].
121. U. -G. Meißner and W. Wang, *Phys. Lett. B* **730**, 336 (2014) [arXiv:1312.3087 [hep-ph]].
122. K. M. Watson, *Phys. Rev.* **88**, 1163 (1952).
123. O. Bar and M. Golterman, *Phys. Rev. D* **87**, 014505 (2013) [arXiv:1209.2258 [hep-lat]].
124. J. Gasser and U. G. Meißner, *Nucl. Phys. B* **357**, 90 (1991).
125. J. A. Oller, E. Oset and J. E. Palomar, *Phys. Rev. D* **63**, 114009 (2001) [hep-ph/0011096].
126. S. Gardner and U. -G. Meißner, *Phys. Rev. D* **65**, 094004 (2002) [hep-ph/0112281].
127. U. -G. Meißner and J. A. Oller, *Nucl. Phys. A* **679**, 671 (2001) [hep-ph/0005253].
128. M. Frink, B. Kubis and U. -G. Meißner, *Eur. Phys. J. C* **25**, 259 (2002) [hep-ph/0203193].
129. J. Bijnens and P. Talavera, *Nucl. Phys. B* **669**, 341 (2003) [hep-ph/0303103].
130. T. A. Lahde and U. -G. Meißner, *Phys. Rev. D* **74**, 034021 (2006) [hep-ph/0606133].
131. Z. -H. Guo, J. A. Oller and J. Ruiz de Elvira, *Phys. Rev. D* **86**, 054006 (2012) [arXiv:1206.4163 [hep-ph]].
132. J. F. Donoghue, J. Gasser and H. Leutwyler, *Nucl. Phys. B* **343**, 341 (1990).
133. M. Jamin, J. A. Oller and A. Pich, *Nucl. Phys. B* **587**, 331 (2000) [hep-ph/0006045].
134. M. Jamin, J. A. Oller and A. Pich, *Nucl. Phys. B* **622**, 279 (2002) [hep-ph/0110193].
135. M. Jamin, J. A. Oller and A. Pich, *Phys. Rev. D* **74**, 074009 (2006) [hep-ph/0605095].
136. V. Bernard and E. Passemar, *Phys. Lett. B* **661**, 95 (2008) [arXiv:0711.3450 [hep-ph]].
137. V. Bernard and E. Passemar, *JHEP* **1004**, 001 (2010) [arXiv:0912.3792 [hep-ph]].
138. F. K. Guo, B. Kubis, U. -G. Meißner, and W. Wang, in preparation.
139. C.-H. Chen and H.-N. Li, *Phys. Lett. B* **561**, 258 (2003) [hep-ph/0209043].
140. B. El-Bennich, A. Furman, R. Kaminski, L. Lesniak, B. Loiseau and B. Moussallam, *Phys. Rev. D* **79**, 094005 (2009) [Erratum-ibid. *D* **83**, 039903 (2011)] [arXiv:0902.3645 [hep-ph]].
141. Z. -H. Zhang, X. -H. Guo and Y. -D. Yang, *Phys. Rev. D* **87**, no. 7, 076007 (2013) [arXiv:1303.3676 [hep-ph]].
142. I. Bediaga, T. Frederico and O. Lourenzo, arXiv:1307.8164 [hep-ph].
143. H. -Y. Cheng and C. -K. Chua, *Phys. Rev. D* **88**, 114014 (2013) [arXiv:1308.5139 [hep-ph]].
144. D. Xu, G. -N. Li and X. -G. He, *Phys. Lett. B* **728**, 579 (2014) [arXiv:1311.3714 [hep-ph]].
145. D. Xu, G. -N. Li and X. -G. He, *Int. J. Mod. Phys. A* **29**, 1450011 (2014) [arXiv:1307.7186 [hep-ph]].
146. H. -Y. Cheng and C. -K. Chua, *Phys. Rev. D* **89**, 074025 (2014) [arXiv:1401.5514 [hep-ph]].
147. Y. Li, arXiv:1401.5948 [hep-ph].
148. W. -F. Wang, H. -C. Hu, H. -n. Li and C. -D. Lü *Phys. Rev. D* **89**, 074031 (2014)

- [arXiv:1402.5280 [hep-ph]].
149. Y. Li, arXiv:1402.6052 [hep-ph].
 150. B. Bhattacharya, M. Gronau and J. L. Rosner, Phys. Lett. B **726**, 337 (2013) [arXiv:1306.2625 [hep-ph]].
 151. J. Charles, A. Le Yaouanc, L. Oliver, O. Pene and J. C. Raynal, Phys. Rev. D **60**, 014001 (1999) [hep-ph/9812358].
 152. M. Beneke and T. Feldmann, Nucl. Phys. B **592**, 3 (2001) [hep-ph/0008255].
 153. C. W. Bauer, D. Pirjol and I. W. Stewart, Phys. Rev. D **67**, 071502 (2003) [hep-ph/0211069].
 154. M. Beneke, Y. Kiyo and D. s. Yang, Nucl. Phys. B **692**, 232 (2004) [hep-ph/0402241].
 155. M. Beneke and D. Yang, Nucl. Phys. B **736**, 34 (2006) [hep-ph/0508250].
 156. M. Diehl, T. Gousset, B. Pire and O. Teryaev, Phys. Rev. Lett. **81**, 1782 (1998) [hep-ph/9805380].
 157. M. V. Polyakov, Nucl. Phys. B **555**, 231 (1999) [hep-ph/9809483].
 158. N. Kivel, L. Mankiewicz and M. V. Polyakov, Phys. Lett. B **467**, 263 (1999) [hep-ph/9908334].
 159. M. Diehl, Phys. Rept. **388**, 41 (2003) [hep-ph/0307382].
 160. Y. -Y. Charng, T. Kurimoto and H. -n. Li, Phys. Rev. D **74**, 074024 (2006) [Erratum-ibid. D **78**, 059901 (2008)] [hep-ph/0609165].
 161. W. Wang, Y. -L. Shen and C. -D. Lu, J. Phys. G **37**, 085006 (2010) [arXiv:0908.2216 [hep-ph]].
 162. X. -W. Kang, B. Kubis, C. Hanhart and U. -G. Meißner, arXiv:1312.1193 [hep-ph].
 163. H. -n. Li and S. Mishima, JHEP **0703**, 009 (2007) [hep-ph/0610120].
 164. M. Gronau and D. London, Phys. Lett. B **253**, 483 (1991).
 165. M. Gronau and D. Wyler, Phys. Lett. B **265**, 172 (1991).
 166. D. Atwood, I. Dunietz and A. Soni, Phys. Rev. Lett. **78**, 3257 (1997) [hep-ph/9612433].
 167. D. Atwood, I. Dunietz and A. Soni, Phys. Rev. D **63**, 036005 (2001) [hep-ph/0008090].
 168. A. Giri, Y. Grossman, A. Soffer and J. Zupan, Phys. Rev. D **68**, 054018 (2003) [hep-ph/0303187].
 169. R. Aaij *et al.* [LHCb Collaboration], Phys. Rev. Lett. **108**, 111602 (2012) [arXiv:1112.0938 [hep-ex]].
 170. T. Aaltonen *et al.* [CDF Collaboration], Phys. Rev. Lett. **109**, 111801 (2012) [arXiv:1207.2158 [hep-ex]].
 171. B. R. Ko [Belle Collaboration], arXiv:1212.1975 [hep-ex].
 172. RAaij *et al.* [LHCb Collaboration], Phys. Lett. B **723**, 33 (2013) [arXiv:1303.2614 [hep-ex]].
 173. W. Wang, Phys. Rev. Lett. **110**, no. 6, 061802 (2013) [arXiv:1211.4539 [hep-ph]].
 174. M. Martone and J. Zupan, Phys. Rev. D **87**, no. 3, 034005 (2013) [arXiv:1212.0165 [hep-ph]].
 175. B. Bhattacharya, D. London, M. Gronau and J. L. Rosner, Phys. Rev. D **87**, 074002 (2013) [arXiv:1301.5631 [hep-ph]].
 176. A. Bondar, A. Dolgov, A. Poluektov and V. Vorobiev, Eur. Phys. J. C **73**, 2476 (2013) [arXiv:1303.6305 [hep-ph]].
 177. C. C. Meca and J. P. Silva, Phys. Rev. Lett. **81**, 1377 (1998) [hep-ph/9807320].
 178. J. P. Silva and A. Soffer, Phys. Rev. D **61**, 112001 (2000) [hep-ph/9912242].
 179. M. Rama, Phys. Rev. D **89**, 014021 (2014) [arXiv:1307.4384 [hep-ex]].
 180. J. Brod and J. Zupan, JHEP **1401**, 051 (2014) [arXiv:1308.5663 [hep-ph]].
 181. K. Trabelsi [Belle Collaboration], arXiv:1301.2033 [hep-ex].

182. J. P. Lees *et al.* [BaBar Collaboration], Phys. Rev. D **87**, no. 5, 052015 (2013) [arXiv:1301.1029 [hep-ex]].
183. RAaaj *et al.* [LHCb Collaboration], Phys. Lett. B **726**, 151 (2013) [arXiv:1305.2050 [hep-ex]].
184. W. Wang, Phys. Rev. D **85**, 051301 (2012) [arXiv:1110.5194 [hep-ph]].
185. W. Wang, AIP Conf. Proc. **1492**, 117 (2012) [arXiv:1209.1244 [hep-ph]].
186. M. Diehl and G. Hiller, JHEP **0106**, 067 (2001) [hep-ph/0105194].
187. M. Diehl and G. Hiller, Phys. Lett. B **517**, 125 (2001) [hep-ph/0105213].
188. C. S. Kim, R. -H. Li and W. Wang, Phys. Rev. D **88**, 034003 (2013) [arXiv:1305.5320 [hep-ph]].
189. Z. -T. Zou, X. Yu and C. -D. Lu, Phys. Rev. D **86**, 094001 (2012) [arXiv:1205.2971 [hep-ph]].
190. Z. -T. Zou and C. -D. Lu, arXiv:1401.1298 [hep-ph].
191. Z. -T. Zou, X. Yu and C. -D. Lu, arXiv:1209.3369 [hep-ph].
192. H. -Y. Cheng, Y. Koike and K. -C. Yang, Phys. Rev. D **82**, 054019 (2010) [arXiv:1007.3541 [hep-ph]].
193. W. Wang, Phys. Rev. D **83**, 014008 (2011) [arXiv:1008.5326 [hep-ph]].
194. R. -H. Li, C. -D. Lu, W. Wang and X. -X. Wang, Phys. Rev. D **79**, 014013 (2009) [arXiv:0811.2648 [hep-ph]].
195. H. -Y. Cheng, C. -K. Chua, K. -C. Yang, Phys. Rev. **D73**, 014017 (2006) [hep-ph/0508104].
196. H. -Y. Cheng, C. -K. Chua, K. -C. Yang and Z. -Q. Zhang, arXiv:1303.4403 [hep-ph].
197. C. -D. Lu, Y. -M. Wang and H. Zou, Phys. Rev. D **75**, 056001 (2007) [hep-ph/0612210].
198. H. -Y. Han, X. -G. Wu, H. -B. Fu, Q. -L. Zhang and T. Zhong, arXiv:1301.3978 [hep-ph].
199. B. Bhattacharya, M. Imbeault and D. London, Phys. Lett. B **728**, 206 (2014) [arXiv:1303.0846 [hep-ph]].
200. I. Bediaga, G. Guerrer and J. M. de Miranda, Phys. Rev. D **76**, 073011 (2007) [hep-ph/0608268].
201. I. Bediaga, D. R. Boito, G. Guerrer, F. S. Navarra and M. Nielsen, Phys. Lett. B **665**, 30 (2008) [arXiv:0709.0075 [hep-ph]].
202. R. Aaaj *et al.* [LHCb Collaboration], Phys. Rev. Lett. **108**, 101803 (2012) [arXiv:1112.3183 [hep-ex]].
203. T. Aaltonen *et al.* [CDF Collaboration], Phys. Rev. Lett. **109**, 171802 (2012) [arXiv:1208.2967 [hep-ex]].
204. V. M. Abazov *et al.* [D0 Collaboration], Phys. Rev. D **85**, 032006 (2012) [arXiv:1109.3166 [hep-ex]].
205. G. Aad *et al.* [ATLAS Collaboration], JHEP **1212**, 072 (2012) [arXiv:1208.0572 [hep-ex]].
206. RAaaj *et al.* [LHCb Collaboration], Phys. Rev. D **87**, 112010 (2013) [arXiv:1304.2600 [hep-ex]].
207. S. Stone and L. Zhang, Phys. Rev. D **79**, 074024 (2009) [arXiv:0812.2832 [hep-ph]].
208. S. Stone and L. Zhang, arXiv:0909.5442 [hep-ex].
209. P. Colangelo, F. De Fazio and W. Wang, Phys. Rev. D **81**, 074001 (2010) [arXiv:1002.2880 [hep-ph]].
210. P. Colangelo, F. De Fazio and W. Wang, Phys. Rev. D **83**, 094027 (2011) [arXiv:1009.4612 [hep-ph]].
211. O. Leitner, J. -P. Dedonder, B. Loiseau and B. El-Bennich, Phys. Rev. D **82**, 076006 (2010) [arXiv:1003.5980 [hep-ph]].

212. R. Fleischer, R. Kneijens and G. Ricciardi, *Eur. Phys. J. C* **71**, 1832 (2011) [arXiv:1109.1112 [hep-ph]].
213. R. Aaij *et al.* [LHCb Collaboration], *Phys. Lett. B* **698**, 115 (2011) [arXiv:1102.0206 [hep-ex]].
214. J. Li *et al.* [Belle Collaboration], *Phys. Rev. Lett.* **106**, 121802 (2011) [arXiv:1102.2759 [hep-ex]].
215. T. Aaltonen *et al.* [CDF Collaboration], *Phys. Rev. D* **84**, 052012 (2011) [arXiv:1106.3682 [hep-ex]].
216. Y. Xie, P. Clarke, G. Cowan and F. Muheim, *JHEP* **0909**, 074 (2009) [arXiv:0908.3627 [hep-ph]].
217. L. Zhang and S. Stone, *Phys. Lett. B* **719**, 383 (2013) [arXiv:1212.6434 [hep-ph]].
218. A. S. Dighe, I. Dunietz and R. Fleischer, *Eur. Phys. J. C* **6**, 647 (1999) [hep-ph/9804253].
219. R. Fleischer, *Phys. Rev. D* **60**, 073008 (1999) [hep-ph/9903540].
220. X. Liu, W. Wang and Y. Xie, arXiv:1309.0313 [hep-ph].
221. C. -H. Chen and H. -N. Li, *Phys. Rev. D* **71**, 114008 (2005) [hep-ph/0504020].
222. X. Liu, Z. -Q. Zhang and Z. -J. Xiao, *Chin. Phys. C* **34**, 937 (2010).
223. X. Liu, H. -n. Li and Z. -J. Xiao, *Phys. Rev. D* **86**, 011501 (2012) [arXiv:1205.1214 [hep-ph]].
224. B. Bhattacharya, A. Datta and D. London, *Int. J. Mod. Phys. A* **28**, 1350063 (2013) [arXiv:1209.1413 [hep-ph]].
225. S. Faller, R. Fleischer and T. Mannel, *Phys. Rev. D* **79**, 014005 (2009) [arXiv:0810.4248 [hep-ph]].
226. G. Aad *et al.* [ATLAS Collaboration], *Phys. Lett. B* **716**, 1 (2012) [arXiv:1207.7214 [hep-ex]].
227. S. Chatrchyan *et al.* [CMS Collaboration], *Phys. Lett. B* **716**, 30 (2012) [arXiv:1207.7235 [hep-ex]].